Electronic Supplementary Material (ESI)

Transmembrane transport of copper(I) by imidazole-functionalised calix[4]arenes

Nathan Renier,[a] Olivia Reinaud,[b] Ivan Jabin,*[c] and Hennie Valkenier*[a]

[a] Université libre de Bruxelles (ULB), Ecole polytechnique de Bruxelles, Engineering Molecular NanoSystems, Brussel, Belgium

[b] Université de Paris Descartes, Laboratoire de Chimie et Biochimie Pharmacologiques et Toxicologiques, Paris, France

[c] Université libre de Bruxelles (ULB), Laboratoire de Chimie Organique, Brussel, Belgium

Table of contents

1. Synthesis

Anhydrous THF was distilled over sodium and benzophenone. The reactions were carried out under inert atmosphere with argon. Thin layer chromatography was performed on silica gel 60 F_{254} coated aluminium sheets. Compounds were revealed under UV light or with $KMnO_4$. Column chromatography was performed on silica gel 60 (particle size 35−70 μm). The reactions were monitored by thin layer chromatography or NMR spectroscopy.

Nuclear magnetic resonance spectroscopy: ^1H, ^{13}C and correlation measurements were recorded with a Bruker Avance TM 300 instrument (^1H at 300 MHz) and/or Bruker Varian Unity 600 VNMR system (^1H at 600 MHz) and/or Jeol JNM-ECZ400R Spectrometer (^1H at 400 MHz; also ^{13}C, COSY, HSQC). The multiplicities of the signals were abbreviated as follows: s singlet, d doublet, bd broad doublet, t triplet, dt doublet of triplets, m multiplet. The chemical shifts are in ppm and the coupling constants *J* are in Hz. The solvents used are chloroform-d_1 ($CDCl_3$), acetonitrile-d_3 (CD_3CN). The ^1H residual signals of the solvent were used as reference ($CDCl_3$ 7.26 ppm, CD_3CN 1.94 ppm), as well as the ^{13}C signals of the solvent ($CDCl_3$ 77.16 ppm). The infrared spectra were recorded with a Bruker Alpha FT-IR. The high-resolution mass spectra in positive mode were recorded on a 6520 series Quadripole Time of Flight (QTOF) mass spectrometer from Agilent Technologies, fitted with a multimode ion source.

1.1. Synthesis of **1**

The synthesis of **1** was performed according to a published procedure.[i] The ^1H NMR spectrum (300 MHz, $CDCl_3$, 298 K) shows broad signals as described in the literature (Figure S1).

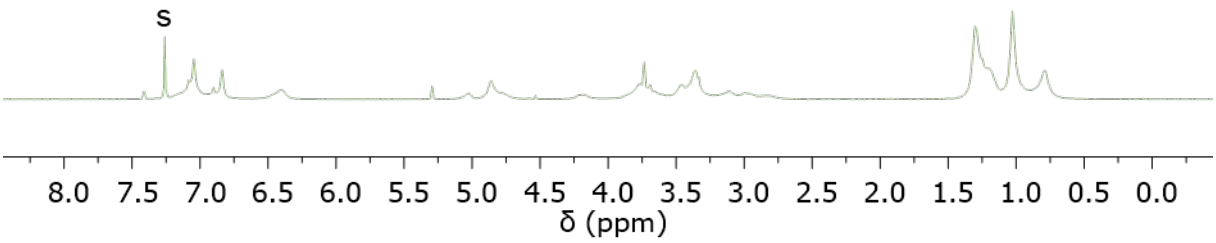

*Figure S1. ^1H NMR spectrum of **1** (300 MHz, $CDCl_3$, 298 K). Residual solvent signal is labelled "s".*

1.2. Synthesis and characterisation of **2**

The synthesis of **2** was performed in two steps. The first step was the bis-alkylation of p-^{t}Bu-calix[4]arene with 1-bromopropane, to yield compound **2b**. This reaction was performed according to a published procedure.[ii] The second step was the alkylation of the remaining phenol groups in condition identical to the alkylation of **1**.

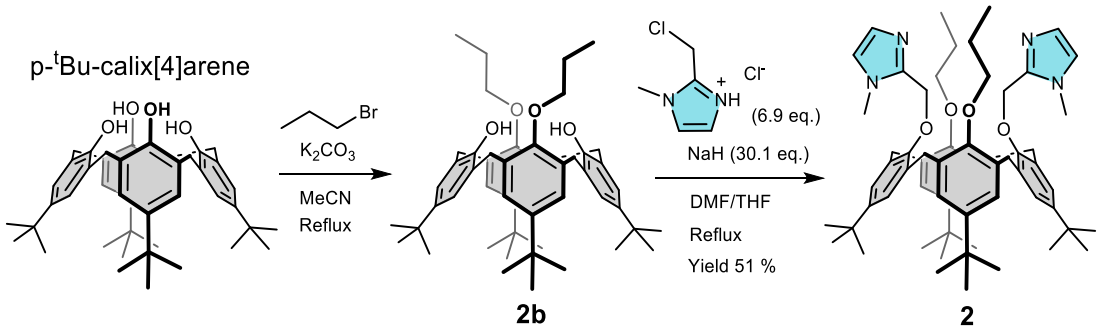

In a 100 mL round bottom flask, calixarene **2b** (82 mg, 0.11 mmol, 1.0 equiv.) was stirred in anhydrous THF (3.2 mL) with NaH (60% dispersion in mineral oil, 134.5 mg, 3.36 mmol, 30.1 equiv.) for 30 minutes under inert atmosphere. 2-(chloromethyl)-1-methyl-1H-imidazole hydrochloride (101.0 mg, 0.77 mmol, 6.9 equiv.) dissolved in anhydrous DMF (0.8 mL) was then added. The mixture was stirred at reflux for 24h under inert atmosphere. After reaction, the mixture was brought to room temperature and quenched with EtOH (0.5 mL). The solvent was evaporated under reduced pressure. The residue was dissolved in DCM (20 mL) and then washed with water (2x10 mL). The organic layer was evaporated under reduced pressure. The crude product was purified by flash chromatography (DCM/MeOH 95:5 v/v). The resulting product was triturated with MeOH (5 mL) and then washed with H_2O to remove the residual complexed Na^+, affording calixarene **2** (52.7 mg, 0.057 mmol) as a white solid. Yield 51 %.
^{1}H NMR (400 MHz, $CDCl_3$, 298 K): δ (ppm) = 0.78 (t, ^3J = 10 Hz, 6H, C**H**$_3$), 0.86 (s, 18H, *t*Bu), 1.28 (s, 18H, *t*Bu), 1.78-1.93 (m, 4H, C**H**$_2$), 3.01 (d, ^2J = 12 Hz, 4H, ArC**H**$_{(eq)}$), 3.45 (s, 6H, NC**H**$_3$), 3.80 (bt, ^3J = 8 Hz, 4H, OC**H**$_2$Et), 4.34 (d, ^2J = 12 Hz, 4H, ArC**H**$_{(ax)}$), 4.82 (s, 4H, OC**H**$_2$Im), 6.49 (s, 4H, Ar**H**), 6.86 (s, 2H, Im**H**), 7.01-7.06 (m, 6H, Ar**H** and Im**H**); ^{13}C NMR (100 MHz, $CDCl_3$, 298 K): δ (ppm) = 9.9 (**C**H$_3$), 23.1 (**C**H$_2$), 30.7 (Ar**C**H$_2$), 31.1 (C(**C**H$_3$)$_3$), 31.7 (C(**C**H$_3$)$_3$), 32.6 (N**C**H$_3$), 33.7 (**C**(CH$_3$)$_3$), 34.1 (**C**(CH$_3$)$_3$), 66.9 (O**C**H$_2$Im), 76.5 (O**C**H$_2$), 121.8 (**Im**H), 124.7 (**Ar**H), 125.5 (**Ar**H), 127.6 (**Im**H), 132.4 (**Ar**CH$_2$), 135.3 (**Ar**CH$_2$), 144.5 (**Ar***t*Bu), 144.8 (**Im**), 145.0 (**Ar***t*Bu), 151.3 (**Ar**OCH$_2$Im), 154.7 (**Ar**OPropyl); IR: ν (cm^{-1}) = 1479, 1361, 1295, 1122, 1042, 977 ; HRMS (ESI): calculated for $C_{60}H_{81}N_4O_4^+$ [M+H$^+$]: 921.6257, measured: 921.6280; mp 253 °C (decomposition).

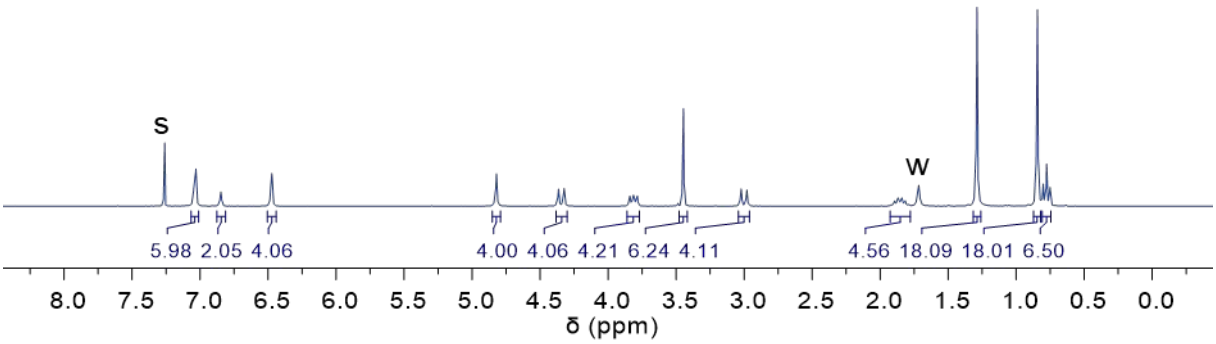

*Figure S2. ^{1}H NMR spectrum of **2** (400 MHz, $CDCl_3$, 298 K). Residual solvent and water signals are labelled "s" and "w".*

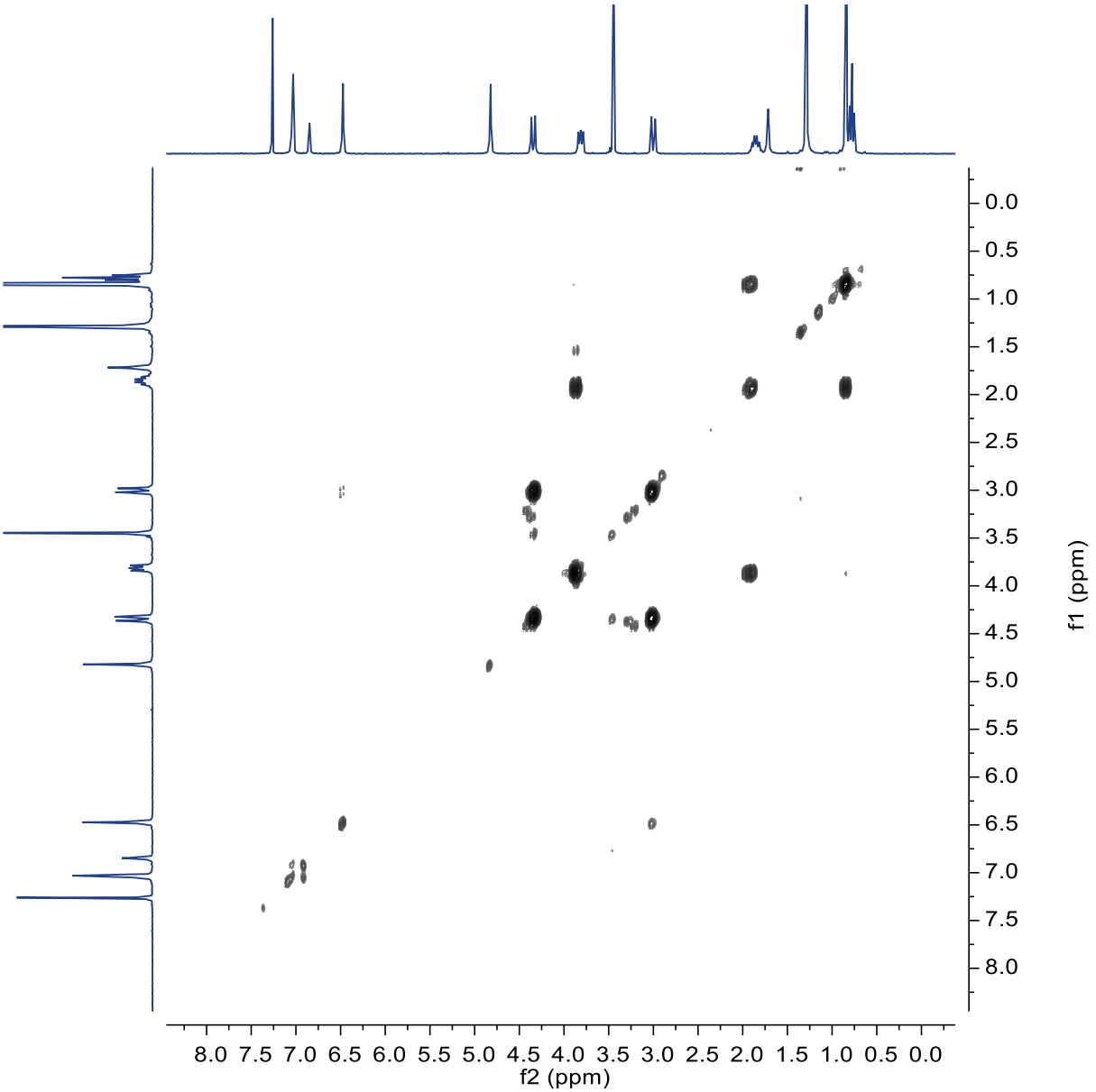

*Figure S3. Correlation spectroscopy (COSY) of **2** (400 MHz, $CDCl_3$, 298 K).*

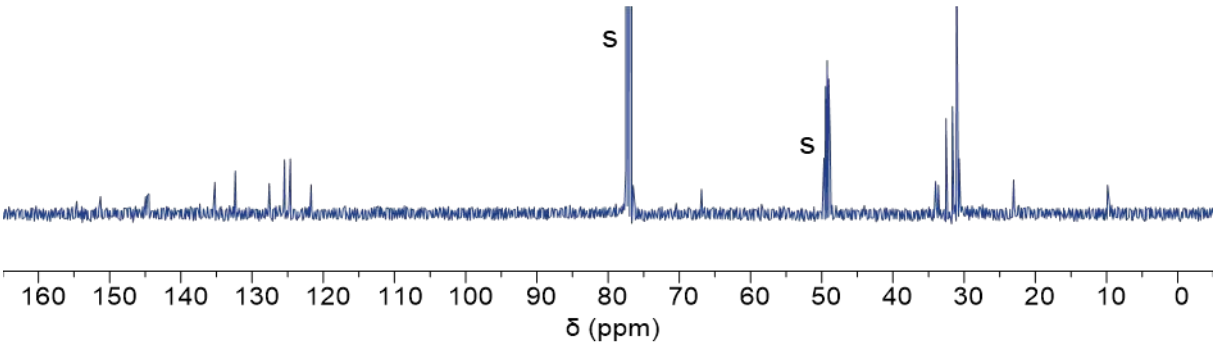

*Figure S4. ^{13}C NMR of **2** (100 MHz, $CDCl_3$, 298 K). Residual solvent signals are labelled "s".*

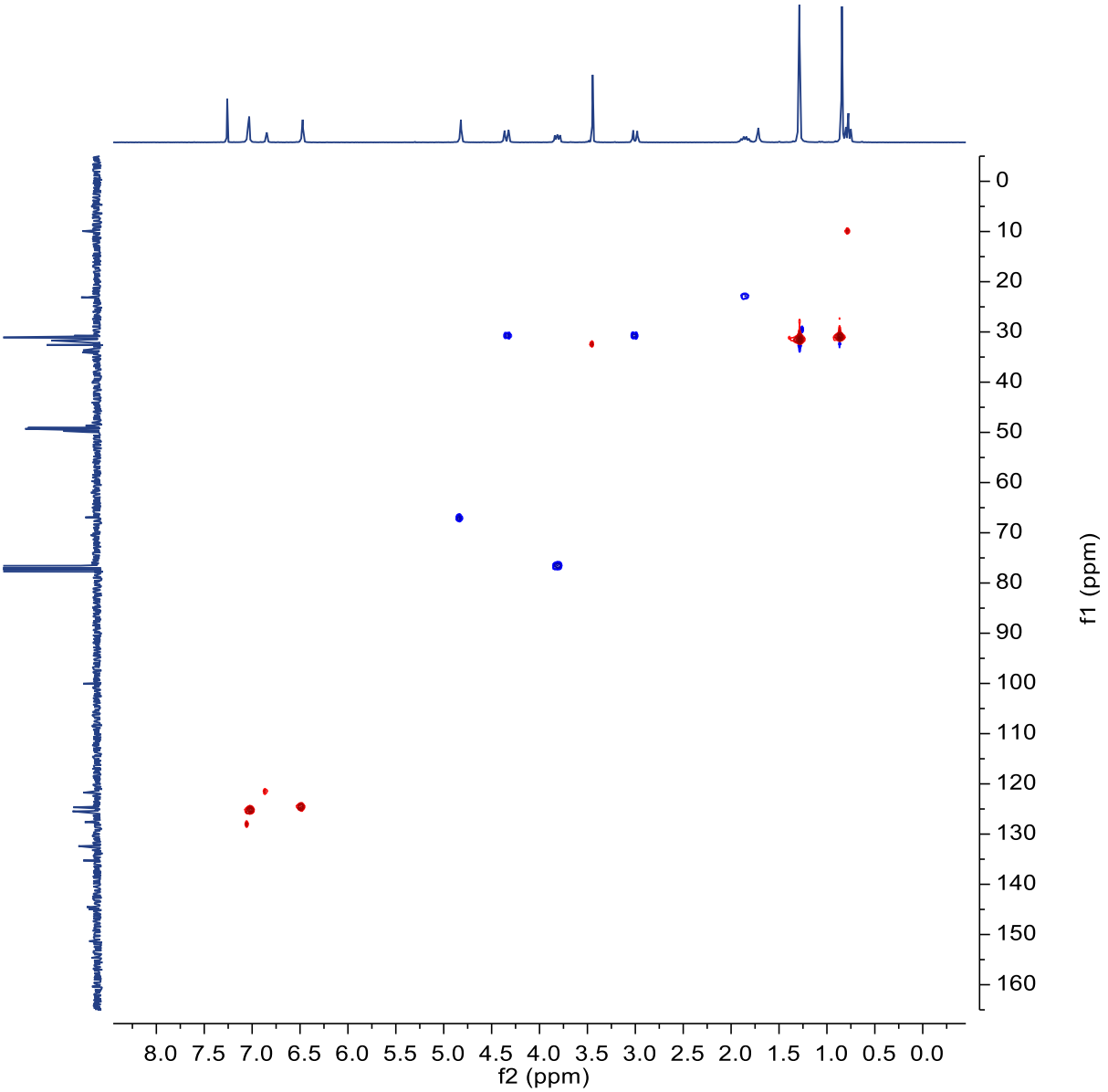

Figure S5. Heteronuclear single quantum coherence spectroscopy (HSQC) of ***2*** *(400 MHz, $CDCl_3$, 298 K).*

1.3. Synthesis and characterisation of **3**

The synthesis of **3** was performed in two steps. The first step was the bis-alkylation of **p-^{t}Bu-**calix[4]arene with 1-bromopentane, to obtain compound **3b**. This reaction was performed according to the same procedure as described for **2b**.[ii] The second step is the alkylation of the remaining phenol groups in conditions identical to the alkylation of **1**.[i]

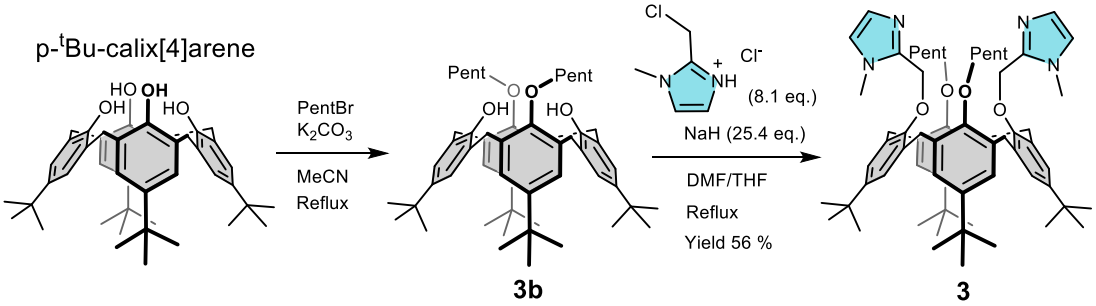

In a 100 mL round bottom flask, calixarene **3b** (352.4 mg, 0.45 mmol, 1.0 equiv.) was stirred in anhydrous THF (10.0 mL) with NaH (60% dispersion in mineral oil, 453.8 mg, 11.3 mmol, 25.4 equiv.) for 30 minutes under inert atmosphere. 2-(chloromethyl)-1-methyl-1H-imidazole hydrochloride (475.3 mg, 3.64 mmol, 8.2 equiv.) dissolved in anhydrous DMF (2.5 mL) was added. The mixture was stirred at reflux for 24h under inert atmosphere. After reaction, the mixture was brought to room temperature and quenched with EtOH (1 mL). The solvent was evaporated under reduced pressure. The residue was dissolved in DCM (100 mL) and then washed with water (2x30 mL). The organic layer was evaporated under reduced pressure. The crude product was purified by flash chromatography (DCM/MeOH 95:5 v/v), affording calixarene **3** (246.0 mg, 0.25 mmol) as a white solid. Yield 56 %.

^{1}H NMR (400 MHz, $CDCl_3$, 298 K): δ (ppm) = 0.86 (s, 18H, *t*Bu), 0.93 (t, ^3J = 8 Hz, 6H, C**H**$_3$), 1.08-1.18 (m, 4H, EtC**H**$_2$), 1.21-1.35 (m, 22 H, *t*Bu and CH_3C**H**$_2$), 1.80-1.92 (m, 4H, OCH_2C**H**$_2$), 2.99 (d, ^2J = 12 Hz, 4H, ArC**H**$_{(eq)}$), 3.46 (s, 6H, NC**H**$_3$), 3.85 (bt, ^3J = 8 Hz, 4H, OC**H**$_2$), 4.33 (d, ^2J = 12 Hz, 4H, ArC**H**$_{(ax)}$), 4.83 (s, 4H, OC**H**$_2$Im), 6.49 (s, 4H, Ar**H**), 6.84 (s, 2H, Im**H**), 6.99-7.05 (m, 6H, Ar**H** and Im**H**); ^{13}C NMR (100 MHz, $CDCl_3$, 298 K): δ (ppm) = 14.7 (**C**H_3), 23.1 (CH_3**C**H_2), 28.4 (Et**C**H_2), 29.9 (OCH_2**C**H_2), 31.0 (Ar**C**H_2), 31.3 (C(**C**H_3)$_3$), 31.8 (C(**C**H_3)$_3$), 32.8 (N**C**H_3), 33.8 (**C**(CH$_3$)$_3$), 34.1 (**C**(CH$_3$)$_3$), 67.3 (O**C**H_2Im), 75.2 (O**C**H_2), 121.6 (**Im**H), 124.8 (**Ar**H), 125.5 (**Ar**H), 128.5 (**Im**H), 132.9 (**Ar**CH_2), 135.2 (**Ar**CH_2), 144.7 (**Ar***t*Bu), 144.8 (**Im**), 145.0 (**Ar***t*Bu), 151.7 (**Ar**OCH_2Im), 154.6 (**Ar**OPentyl); IR: ν (cm^{-1}) = 1480, 1361, 1299, 1285, 1122, 993, 946; MS (ESI): calculated for $C_{64}H_{89}N_4O_4^+$ [M+H$^+$]: 977.6878, measured: 977.6865; mp 220 °C.

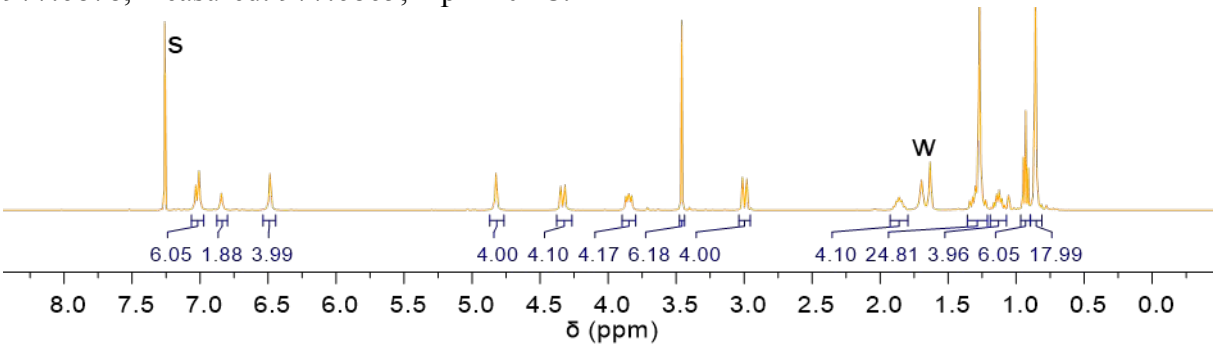

*Figure S6. ^{1}H NMR spectrum of **3** (400 MHz, $CDCl_3$, 298 K). Residual solvent and water signals are labelled "s" and "w".*

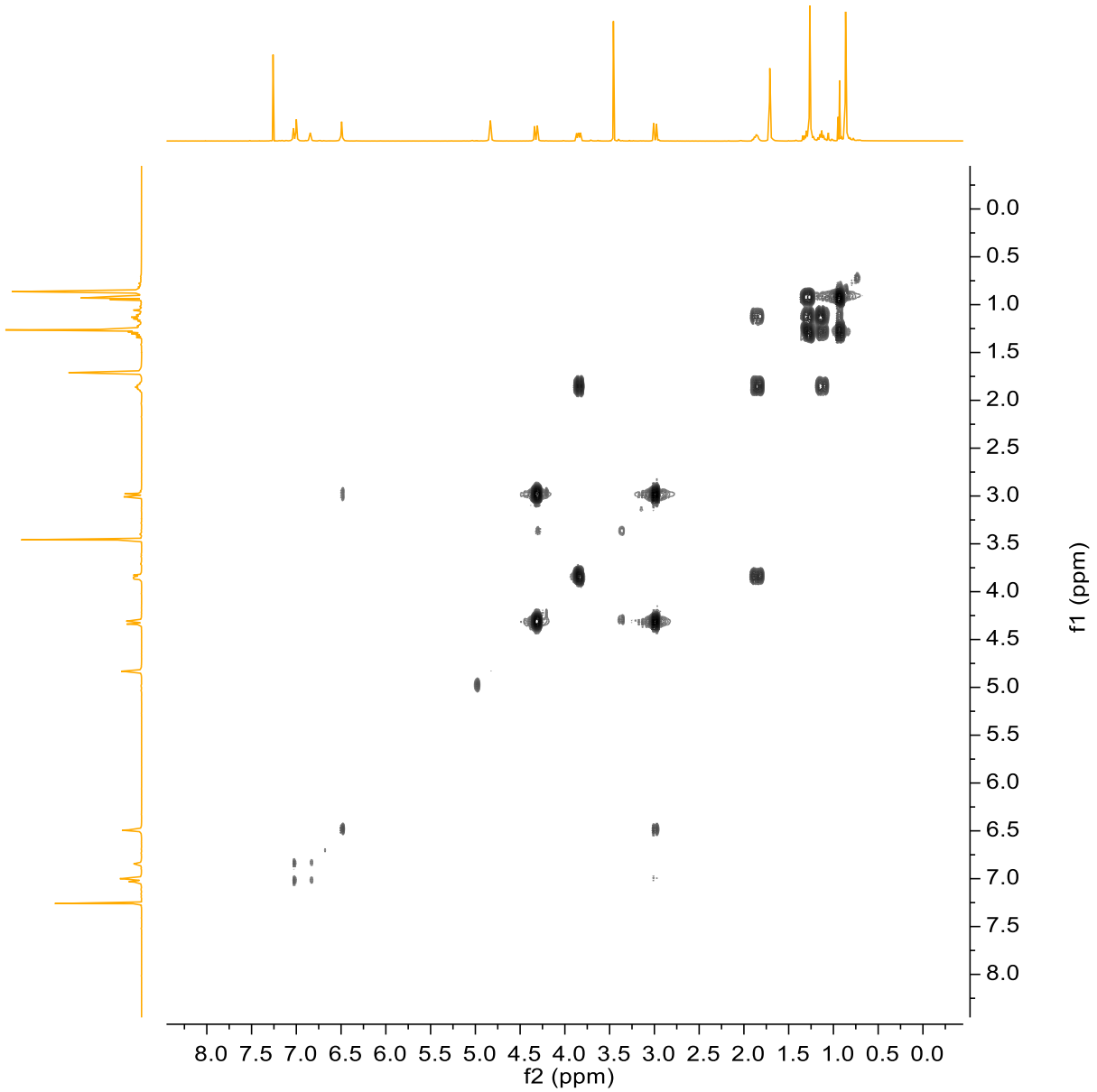

*Figure S7. Correlation spectroscopy (COSY) of **3** (400 MHz, $CDCl_3$, 298 K).*

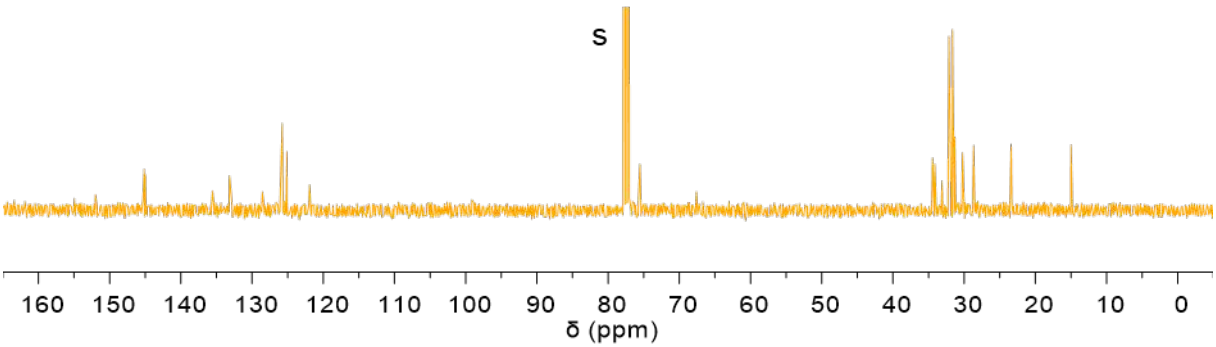

*Figure S8. ^{13}C NMR of **3** (100 MHz, $CDCl_3$, 298 K). Residual solvent signals are labelled "s".*

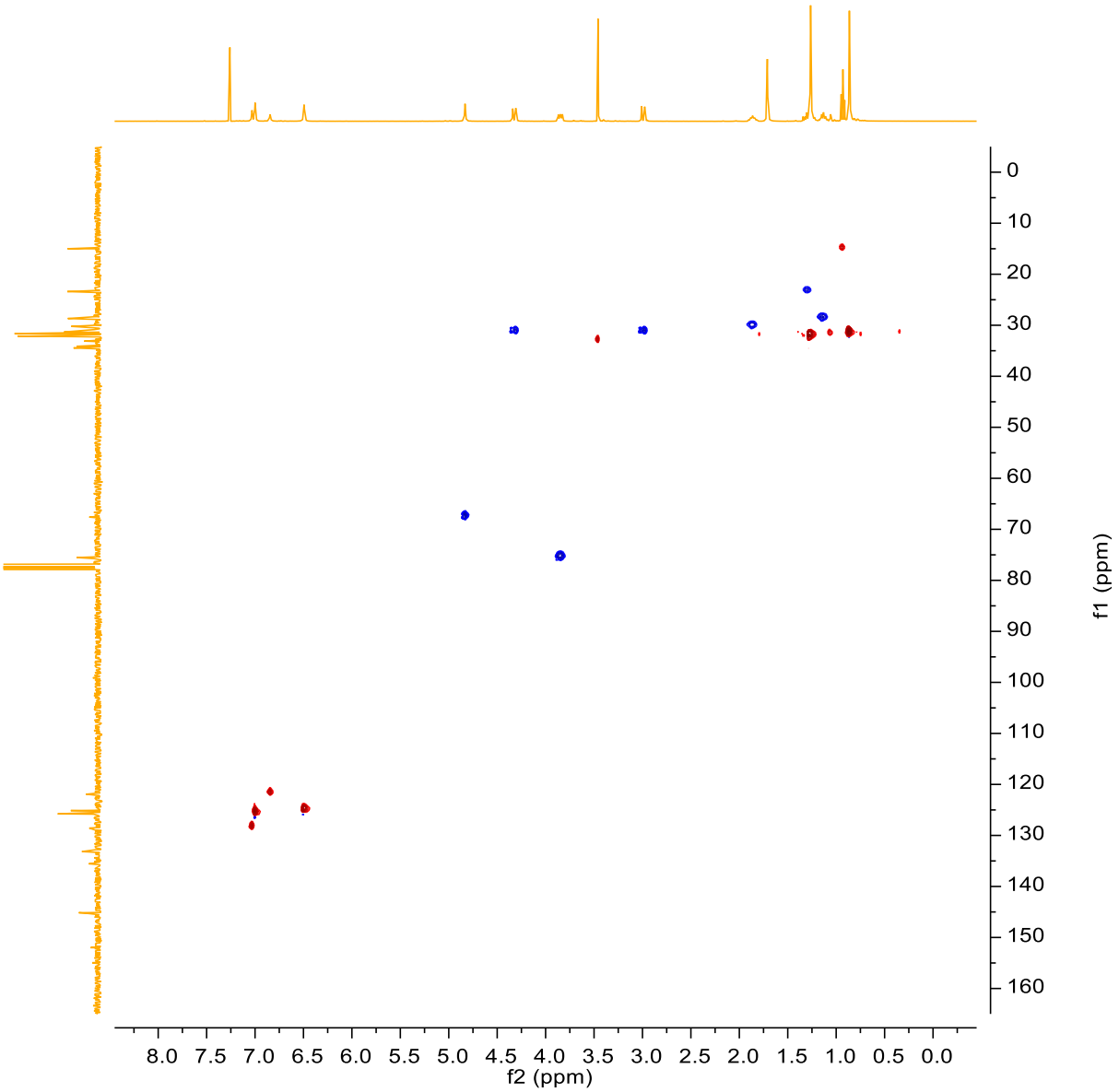

Figure S9. Heteronuclear single quantum coherence spectroscopy (HSQC) of ***3*** *(400 MHz, $CDCl_3$, 298 K).*

1.4. Synthesis and characterisation of **4**

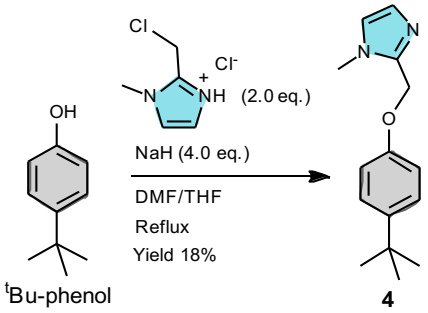

In a 100 mL round bottom flask, ^{t}Bu-phenol (100.0 mg, 0.67 mmol, 1.0 equiv.) was stirred in anhydrous THF (4 mL) with NaH (60% dispersion in mineral oil, 63.9 mg, 2.66 mmol, 4.0 equiv.) for 30 minutes under inert atmosphere. 2-(chloromethyl)-1-methyl-1H-imidazole (149.3 mg, 1.33 mmol, 2.0 equiv.) dissolved in anhydrous DMF (1 mL) and was then added. The mixture was stirred and heated until reflux for 24h under inert atmosphere. The reaction was quenched with EtOH (10 drops). The solvent was evaporated under reduced pressure. The residue was dissolved in DCM and then washed with water (2x10 mL). The organic layer was evaporated under reduced pressure affording **4** (20 mg, 122 mmol) as white solid. Yield 18 %. ^{1}H NMR (400 MHz, $CDCl_3$, 298 K): δ (ppm) = 1.29 (s, 9H, *t*Bu) 3.72 (s, 3H, NC**H**$_3$) 5.13 (s, 2H, OC**H**$_2$), 6.89 (bd, ^{3}J = 0.8 Hz, 1H, Im**H**) 6.97 (dt, ^{3}J = 8.9 Hz and ^{4}J = 3.0 Hz, 2H, Ar**H**) 7.00 (bd, ^{3}J = 0.8 Hz, 1H, Im**H**) 7.31 (dt, ^{3}J = 9.0 Hz and ^{4}J = 2.8 Hz, 2H, Ar**H**); ^{13}C NMR (100 MHz, $CDCl_3$, 298 K) δ (ppm) = 31.6 (C(**C**H$_3$)$_3$), 33.2 (N**C**H$_3$), 34.2 (**C**(CH$_3$)$_3$), 62.7 (O**C**H$_2$), 114.4 (**Ar**H), 122.4 (**Im**H), 126.5 (**Ar**H), 127.9 (**Im**H), 144.3 (**Im** or **Ar^{t}Bu**), 156 (**ArO**), one signal missing; IR : ν (cm^{-1}) = 1464, 1448, 1364, 1285, 1122, 985; MS (ESI): Calculated for $C_{15}H_{21}N_2O^+$ [M+H$^+$]: 245.1648, measured: 245. 1637; mp 201 °C.

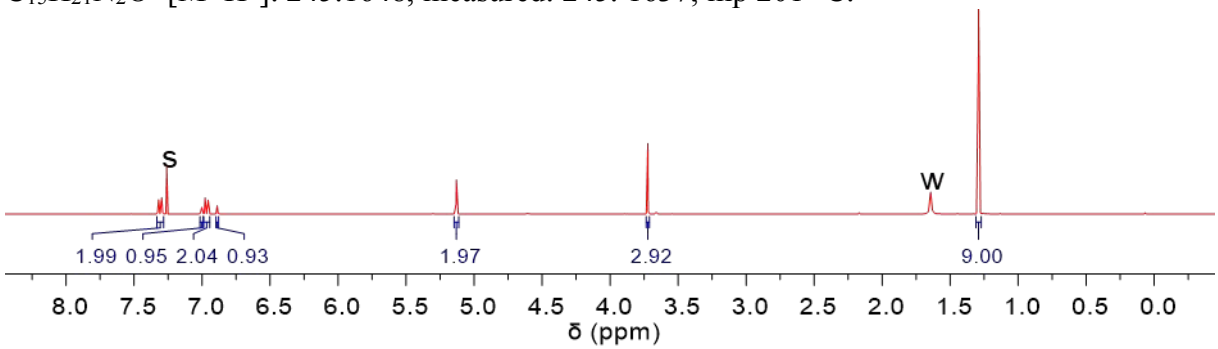

Figure S10. ^{1}*H NMR spectrum of* ***4*** *(400 MHz, $CDCl_3$, 298 K). Residual solvent and water signals are labelled "s" and "w".*

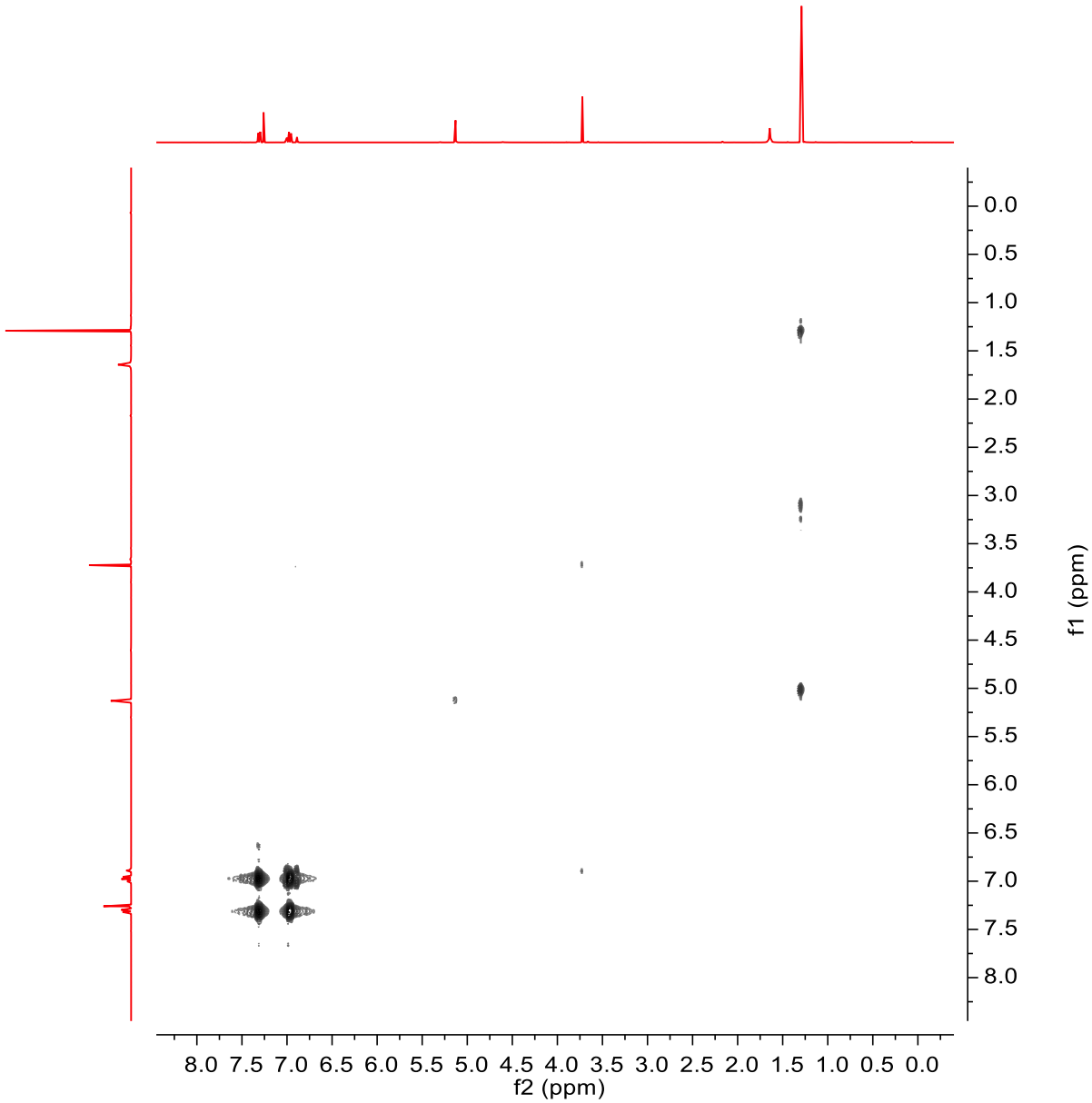

Figure S11. Correlation spectroscopy (COSY) of ***4*** *(400 MHz, $CDCl_3$, 298 K).*

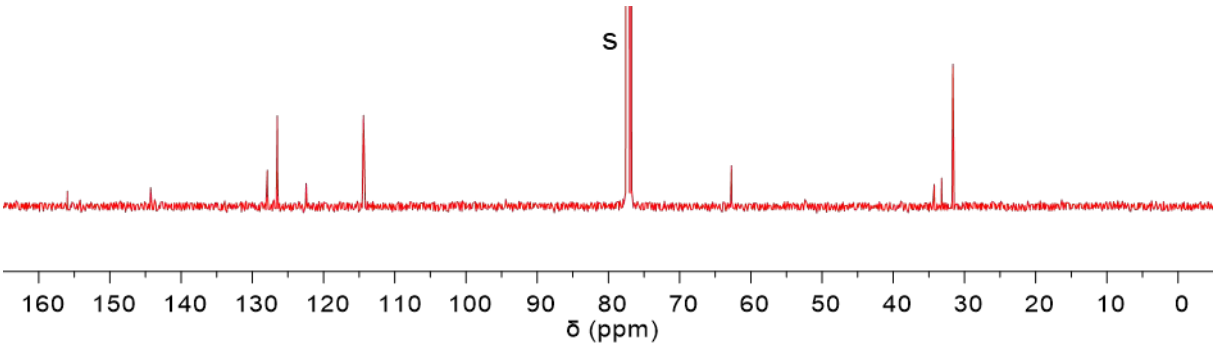

Figure S12. ^{13}C NMR of ***4*** *(400 MHz, $CDCl_3$, 298 K). Residual solvent signal is labelled "s".*

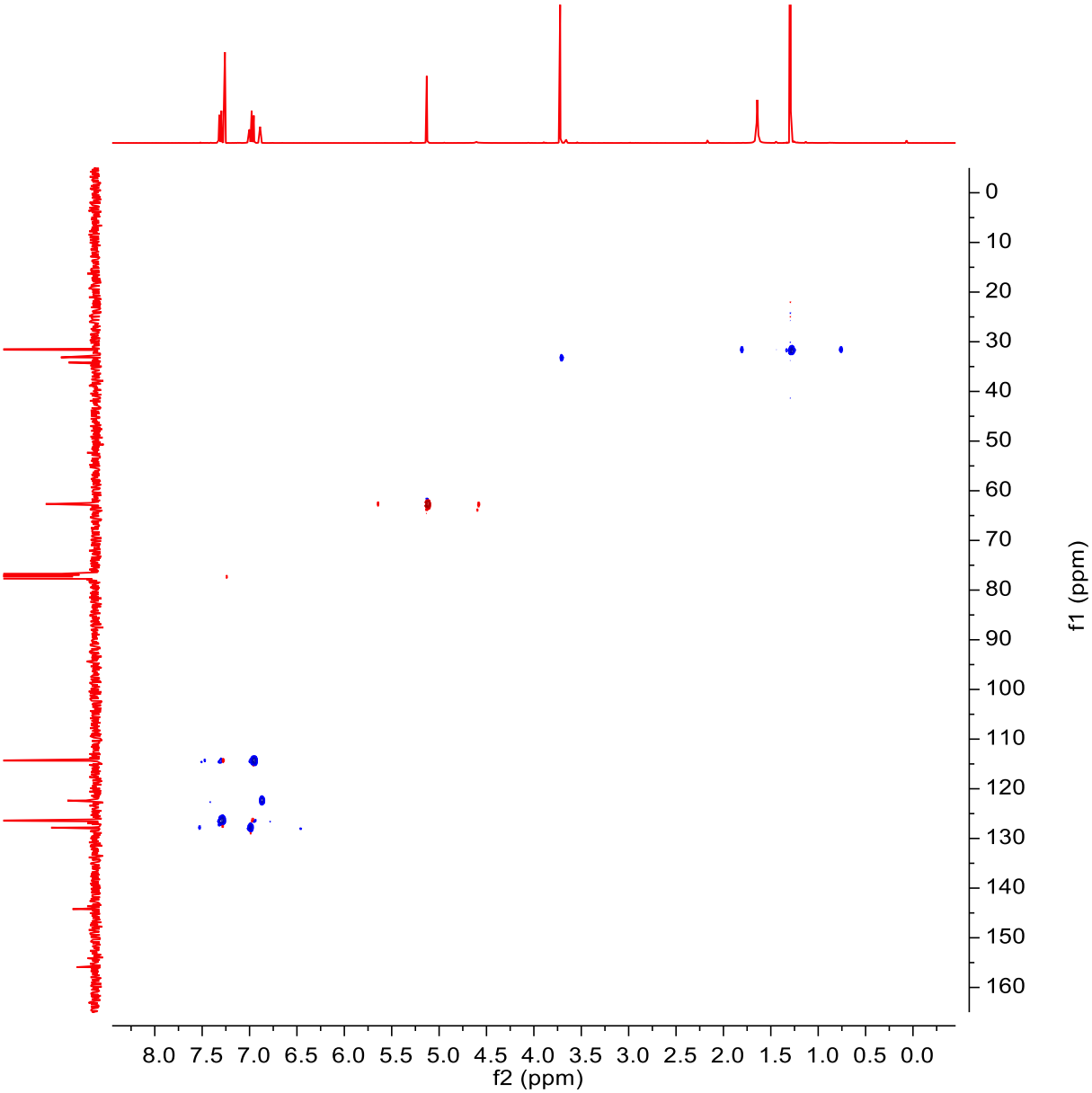

Figure S13. Heteronuclear single quantum coherence spectroscopy (HSQC) of ***4*** *(400 MHz, $CDCl_3$, 298 K).*

2. Cation complexation studies by ^{1}H NMR

2.1. Extraction studies with **2**

In order to evaluate the ability of **2** to extract cations from an aqueous solution, ^{1}H NMR extraction studies were conducted in $CDCl_3$ at 298 K. These ^{1}H NMR measurements were performed on a Jeol JNM-ECZ400R spectrometer (^{1}H, 400 MHz). Parameters for the measurements were a 90° pulse (6.8 µs), acquisition time 3 s, relaxation delay 15 s, 32 scans. 600 µL of 0.5 mM solutions of **2** in deacidified $CDCl_3$ were mixed in NMR tubes with 600 µL of 0.5 mM aqueous solutions of chloride species (HCl, NaCl, KCl, CuCl, $CuCl_2$, and $CuCl_2$ with 1mM sodium ascorbate) and then manually shaken until an emulsion was formed. The shaking was repeated after 24h and the phases were allowed to separate. The data in Figure S14 were recorded 24 h after the beginning of the experiment. Further shaking and stirring to mix the phases did not give any different results.

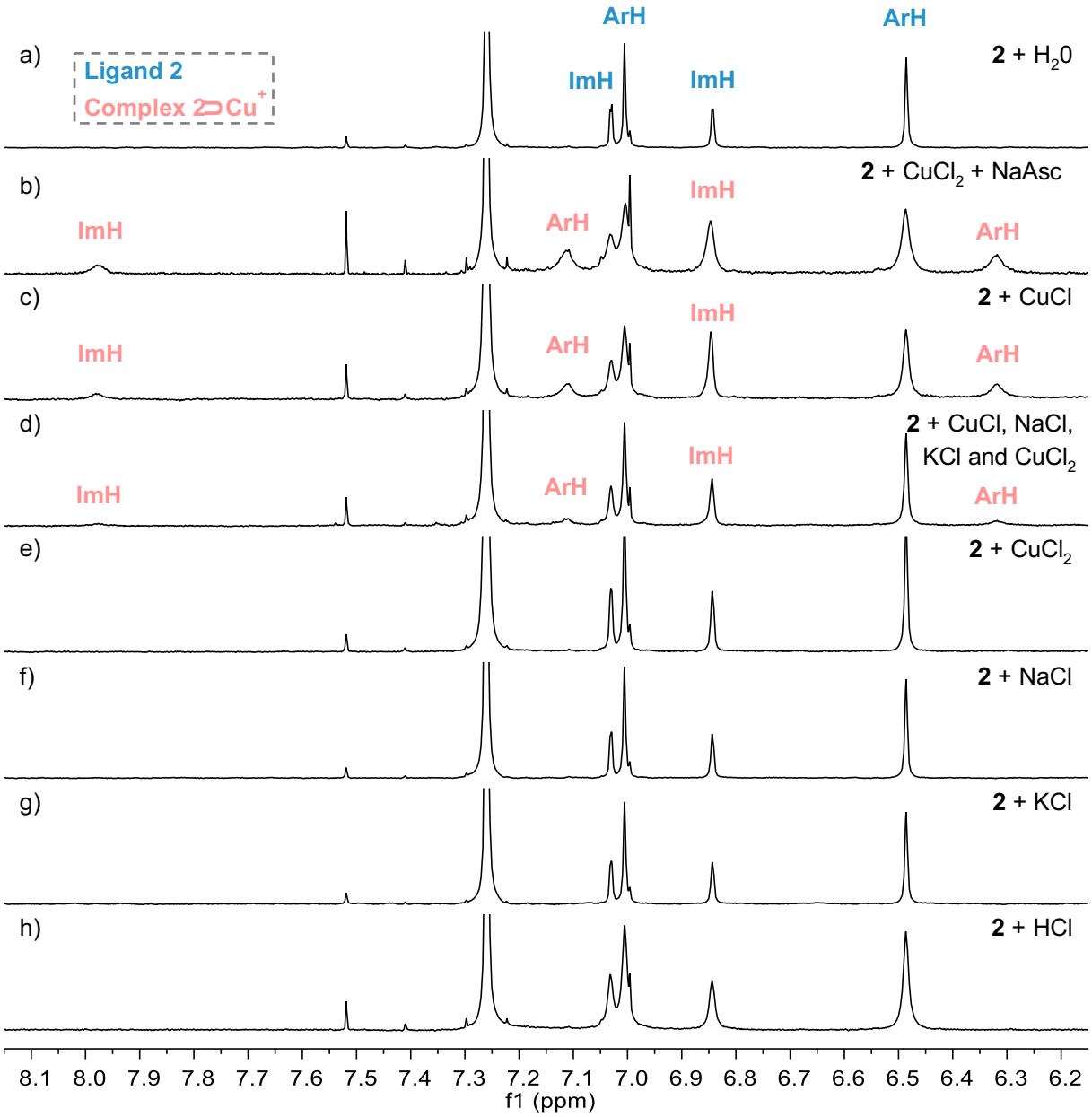

*Figure S14. Results of the extraction studies of cations from H_2O into $CDCl_3$ by receptor **2**. Partial ^{1}H NMR spectra (400 MHz, 298 K) of 600 µL of **2** (0.5 mM) in $CDCl_3$ after addition of 600 µL of aqueous solutions (0.5 mM for all the chloride species) of a) H_2O, b) $CuCl_2$ and sodium ascorbate (1.0 mM), c) CuCl, d) CuCl, NaCl, KCl, $CuCl_2$, e) $CuCl_2$, f) NaCl, g) KCl, h) HCl.*

In order to confirm that the new NMR signature (Figure S14b-d) corresponds to that of **2**⊃Cu^+, this complex was synthesized by adding 2 equivalents of $Cu(CH_3CN)_4PF_6$ (1.2 mM) to **2** in CD_3CN. The solvent mixture was then evaporated and the resulting solid was dissolved in $CDCl_3$, giving the complex [**2**⊃Cu^+]PF_6^-. To form the complex [**2**⊃Cu^+]Cl^-, 2 equivalents of TBACl in $CDCl_3$ (0.5 mM) were added, resulting in the spectrum shown in Figure S15b.

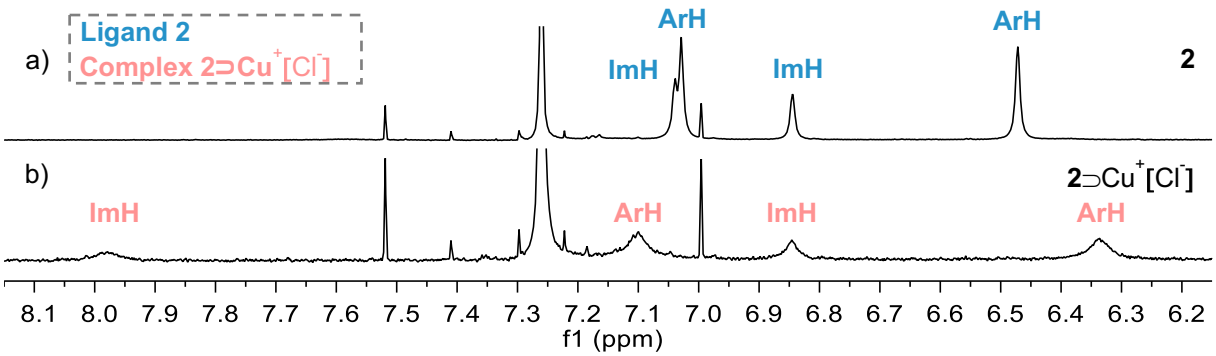

*Figure S15. Partial ^1H NMR spectra ($CDCl_3$, 400 MHz, 298 K) of **2** (0.5 mM) and its Cu^+ complexes: a) **2**; b [**2**⊃Cu^+]Cl^-.*

Figure S15b shows a signature of the complex [**2**⊃Cu^+]Cl^- that is identical to that observed in the extraction studies, confirming that **2** is able to selectively extract Cu^+ from an aqueous phase into $CHCl_3$.

2.2. ^1H NMR spectra of cation complexes of **1**, **2** and **3**

The ability of calixarenes **1**-**3** to bind Cu^+, Na^+, and K^+ in organic solvents was evaluated by ^1H NMR spectroscopy in a 4:1 mixture of $CD_3CN/CDCl_3$. Complexation studies were conducted by separate addition of salts solutions of NaBarf (tetrakis[3,5-bis(trifluoromethyl)phenyl] borate), KPF_6, and $Cu(I)(CH_3CN)_4BF_4$ in CD_3CN to different solutions of **1**, **2** and **3**. Stock solutions of calixarene (**1**, **2** or **3**) were prepared in a mixture of deuterated solvents ($CD_3CN/CDCl_3$ 4:1) and then titrated with the salt or acid solutions (prepared in the receptor stock solutions) until the ^1H NMR signals showed no significant changes anymore.

^1H NMR measurements were performed on a Varian Unity 600 VNMR system (^1H, 600 MHz) and a Varian VNMRS 400 VNMR system (^1H, 400 MHz) at 298K. Parameters for the measurements were a 90° pulse, acquisition time 3 s, relaxation delay 15 s, 8 scans.

The quantitative formation of their complexes with $Cu(I)(CH_3CN)_4BF_4$ and NaBarf was observed upon addition of only 1 eq. of salt, indicating an affinity higher than 10^5 M^{-1} (Figures S16-S18). The low affinity of **2** for KPF_6 allowed the quantification of a K_a, see section 2.3 (Figure S19-20). The ^1H NMR spectra of the free ligands **1**, **2** and **3** and the complexes are shown in Figure S16-18.

On the ^1H NMR spectrum of **2**⊃Cu^+, the difference of chemical shifts between the two ArH and the two ^{t}Bu signals increased compared to the spectrum of the free ligand from 0.27 to 0.83 ppm (ArH) and from 0.20 to 0.56 ppm (^{t}Bu) (Figure 17b and a). This implies that the Cu^+ complex is in a more pinched conformation than the free ligand. The aromatic units linked to the propyl groups are believed to be upright and parallel to each other and the aromatic units

linked to the imidazole groups are tilted towards the center of the small rim. As the interaction with the Cu^+ occurs specifically with the imidazole groups, fixing their conformation upon binding Cu^+ is likely to be responsible for the conformational changes observed. In contrast, the difference of chemical shifts between the two ArH of **2**⊃Na^+, decreased compared to the free ligand **2** from 0.27 to 0.03 ppm, and the ^{t}Bu signals of **2**⊃Na^+ are overlapping each other (Figure 17c), which indicates that all the aromatic units are oriented similarly and the calixarene scaffold is in a straight cone conformation. Upon complexation of K^+, **2** showed similar conformational changes as those of Na^+ (Figure 17 d): only one ArH signal and one ^{t}Bu signal were observed on the ^{1}H NMR spectrum of the K^+ complex, which again indicates a straight cone conformation.

These observations suggest that Cu^+ interacts with **2** in a different way than Na^+ and K^+ do. The last two appear to interact with the lone pairs of the oxygen atoms on the small rim of **2**, resulting in a straight cone conformation,[iii] while the lone pair on the nitrogen atom of the imidazole groups is not necessarily involved in the interaction. Thus, in contrast to the interactions between **2** and Cu^+, the interactions with Na^+ and K^+ are not specific to the imidazole groups.

Similar observations were made with the complexes of **1** and **3**, indicating that the length of alkyl chain does not have a significant impact on the binding mode of the cations tested.

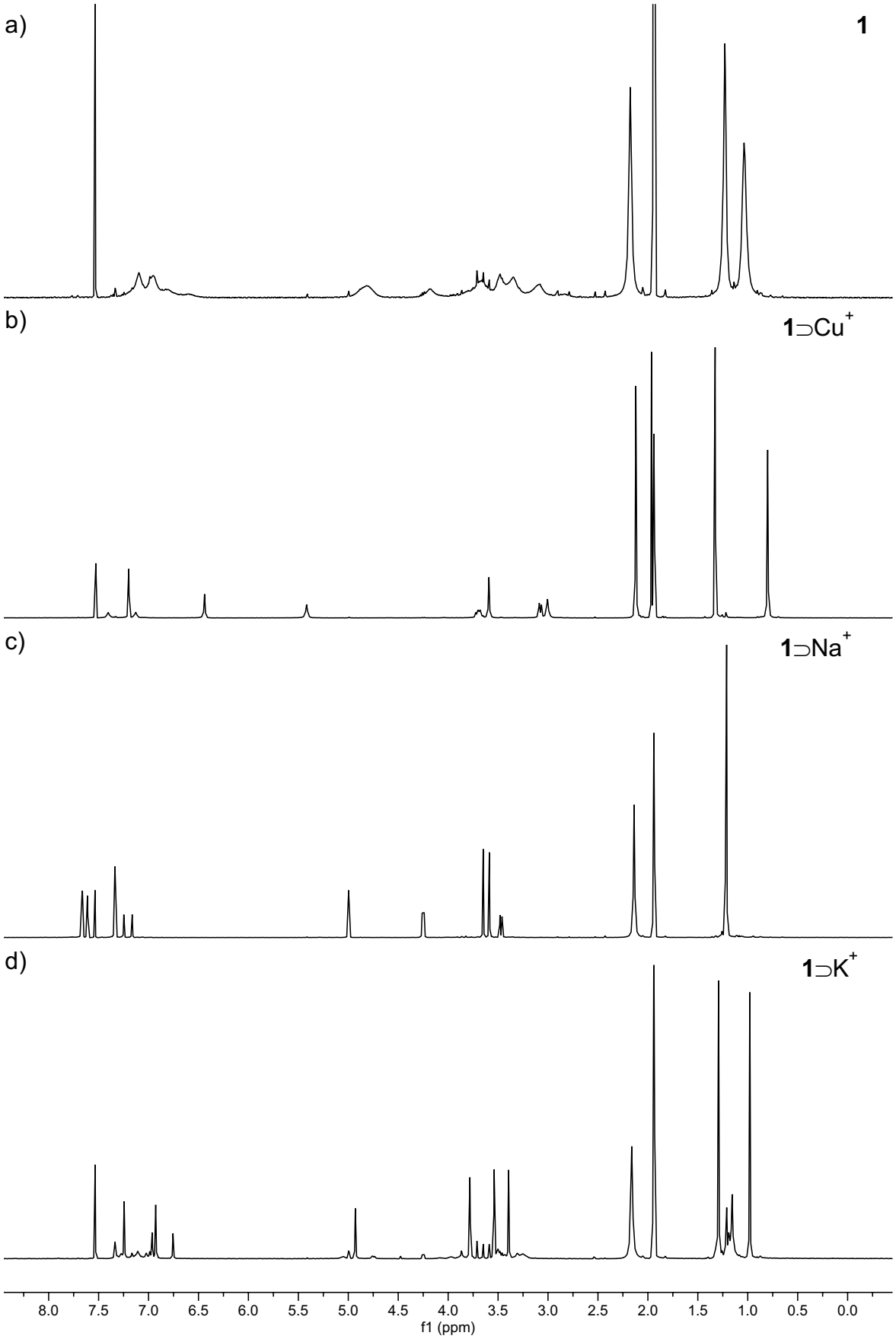

Figure S16. ^{1}*H NMR spectra ($CD_3CN/CDCl_3$ 4:1, 600 MHz, 298 K) of a)* ***1*** *(5 mM), b)* ***1***$\supset Cu^+$ *(1.0 eq. of Cu(I)$(CH_3CN)_4BF_4$ added), c)* ***1***$\supset Na^+$ *(1.1 eq. of NaBarf added) and d)* ***1***$\supset K^+$ *(1.4 eq. of KPF_6 added).*

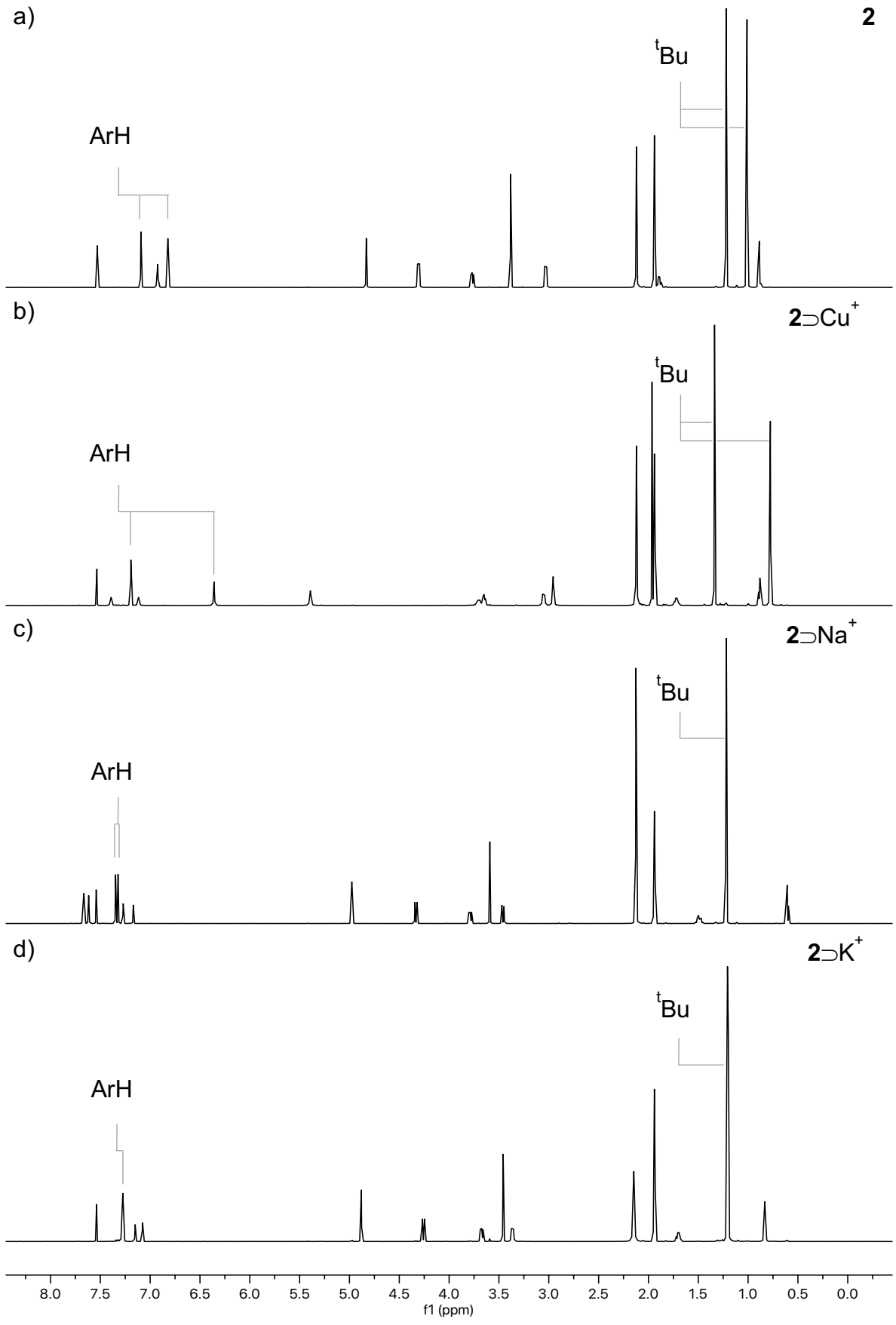

Figure S17. ^{1}*H NMR spectra (*$CD_3CN/CDCl_3$ *4:1, 600 MHz, 298 K) of a)* ***2*** *(5 mM), b)* ***2***$\supset Cu^+$ *(1.0 eq. of* $Cu(I)(CH_3CN)_4BF_4$ *added), c)* ***2***$\supset Na^+$ *(1.3 eq. of NaBarf added) and d)* ***2***$\supset K^+$ *(1.8 eq. of* KPF_6 *added).*

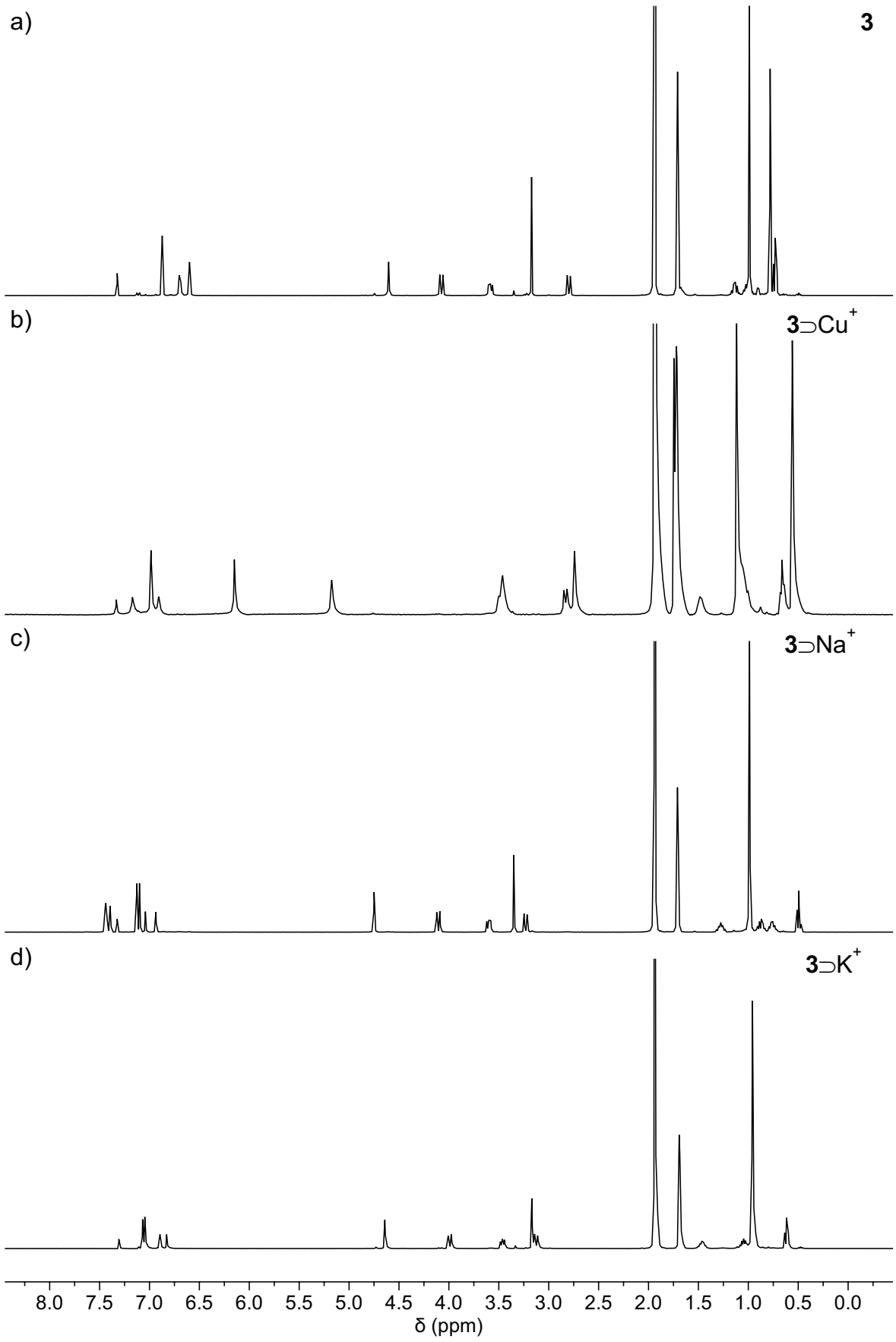

Figure S18. ^{1}*H NMR spectra (*$CD_3CN/CDCl_3$ *4:1, 400 MHz, 298 K) of a)* ***3*** *(5 mM), b)* ***3***$\supset Cu^+$ *(1.0 eq. of* $Cu(I)(CH_3CN)_4BF_4$ *added), c)* ***3***$\supset Na^+$ *(1.0 eq. of NaBarf added) and d)* ***3***$\supset K^+$ *(5.0 eq. of* KPF_6 *added).*

2.3. ^{1}H NMR titration to quantify the affinity of **2** for K^+

In contrast to the interaction of **2** with Cu^+ and Na^+ salts, the K_a of **2** for KPF_6 was low enough to be measured by ^{1}H NMR spectroscopy and the exchange rate between the free receptor and the complex **2**⊃K^+ was slow on the NMR time scale (Figure S19). The variation with the addition of K^+ of chemical shifts of the $ArCH_{(eq)}$, OCH_2Et, $ArCH_{(ax)}$ and ^{t}Bu signals were measured and data were fitted to a 1:1 binding model, resulting in a K_a value of 1930 ± 50 M^{-1} (Figure S20).

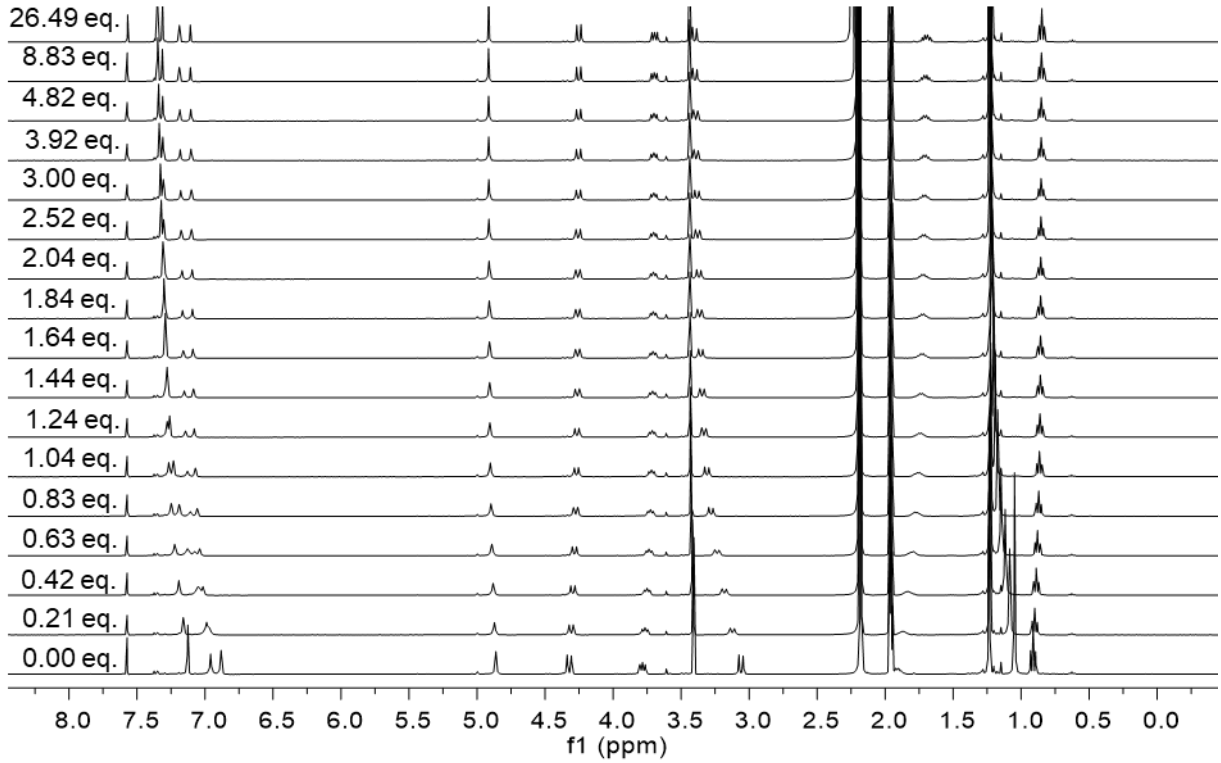

*Figure S19. ^{1}H NMR titration (400 MHz, 298 K) of **2** (4.65 mM in $CD_3CN/CDCl_3$ 4:1) with KPF_6 (246 mM in stock solution of **2**) from 0 to 26.49 equivalents of K^+.*

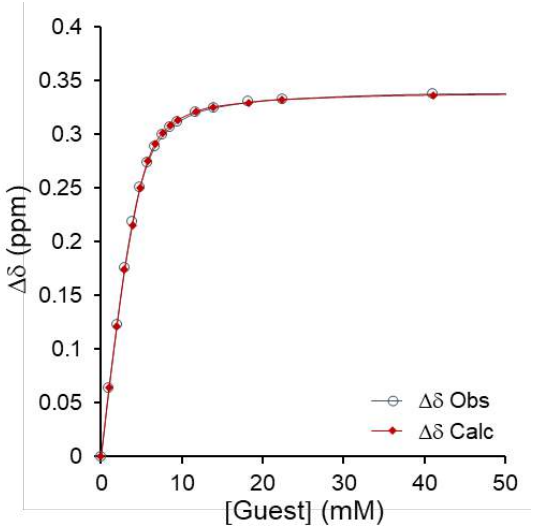

*Figure S20. Observed changes in chemical shift ($ArCH_{(eq)}$, moving from 3.05 to 3.40 ppm) for **2** (4.65 mM in $CD_3CN/CDCl_3$ 4:1) when titrated against potassium (KPF_6 246 mM in stock solution of **2**) at 298 K and calculated changes in chemical shift from the fitting of the $ArCH_{(eq)}$, OCH_2Et, $ArCH_{(ax)}$, and ^{t}Bu signals to a 1:1 binding model using the online tool Bindfit,[iv] giving a binding constant K_a = 1930 ± 50 M^{-1} for the complex **2**⊃K^+.*

2.4. ^{1}H NMR competition studies to determine the affinity of **2** for Cu^+ and Na^+

As mentioned in Section 2.2 the affinity of **2** for Cu^+ and Na^+ is too high to be determined through direct titrations, but competition between K^+, for which the binding affinity has been determined, and Cu^+ or Na^+ could allow to obtain the affinity constants. A stock solution of calixarene **2** was prepared containing an excess of KPF_6 (100 eq.). Solutions of $NaPF_6$ and $Cu(MeCN)_4PF_6$ were prepared using this stock solution. A titration of the **2**⊃K^+ with the Na^+ and Cu^+ salts was performed. After addition of only 1 equivalent of either salt, the signal of **2**⊃K^+ was not observed anymore. Assuming, based on the sensitivity of NMR spectroscopy, that maximum 5% of **2** could still be present as **2**⊃K^+ complex under those conditions, we calculated that the logK_a values of **2** for both Na^+ and Cu^+ are higher than 7. Further increase of the K^+ concentration was limited by KPF_6 solubility in the 4:1 mixture of $CD_3CN/CDCl_3$.

3. Characterization of the dye BCS by optical spectroscopy

Absorption and fluorescence spectroscopy were used to study the optical properties of bathocuproine disulphonate (BCS) upon addition of Cu^+. The absorption was measured from 600 nm to 250 nm with a Shimadzu UV-Vis-NIR UV-3600 spectrometer. The fluorescence measurements were performed with a Horiba FluoroMax 4 spectrometer at 298 K. The excitation was done at the absorption maximum, *i.e.* 282 nm and the emission spectra were measured from 340 nm to 560 nm with slits openings set at 1 nm. The excitation spectra were measured at 394 nm when exciting from 240 nm to 370 nm.

A solution of BCS (3 mL, 10 µM) in a salt buffer (50 mM sodium phosphate at pH 7) was placed in a four-faced quartz cuvette. The BCS solution was titrated with solutions of Cu^+ prepared from 0.5 mM $CuCl_2$ with 1 mM sodium ascorbate in 50 mM sodium phosphate at pH 7 and containing the same concentration of BCS. After each addition, both the absorption and emission spectra were recorded (Figures S21, S22), while the excitation spectra were only recorded at few points during the titration. The emission spectra of a titration with a 10-fold higher concentration of BCS (0.1 mM, Figure S23) were also measured.

3.1. Absorption spectroscopy

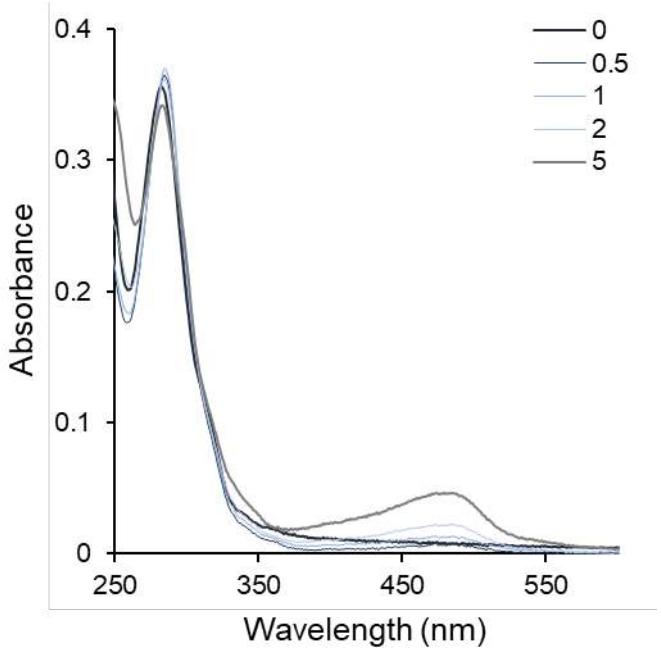

Figure S21. Absorption spectra of a 10 µM BCS solution (in a 50 mM sodium phosphate buffer at pH 7) titrated with a solution of 50 µM $CuCl_2$ and 100 µM sodium ascorbate (in a stock solution of BCS). The added amount is expressed in number of equivalents of Cu^+ relative to BCS.

3.2. Fluorescence spectroscopy

When exciting at the absorption band maxima, 282 nm, an emission band centred around 394 nm was observed. The emission intensity decreased upon addition of Cu^+ to the BCS solution.

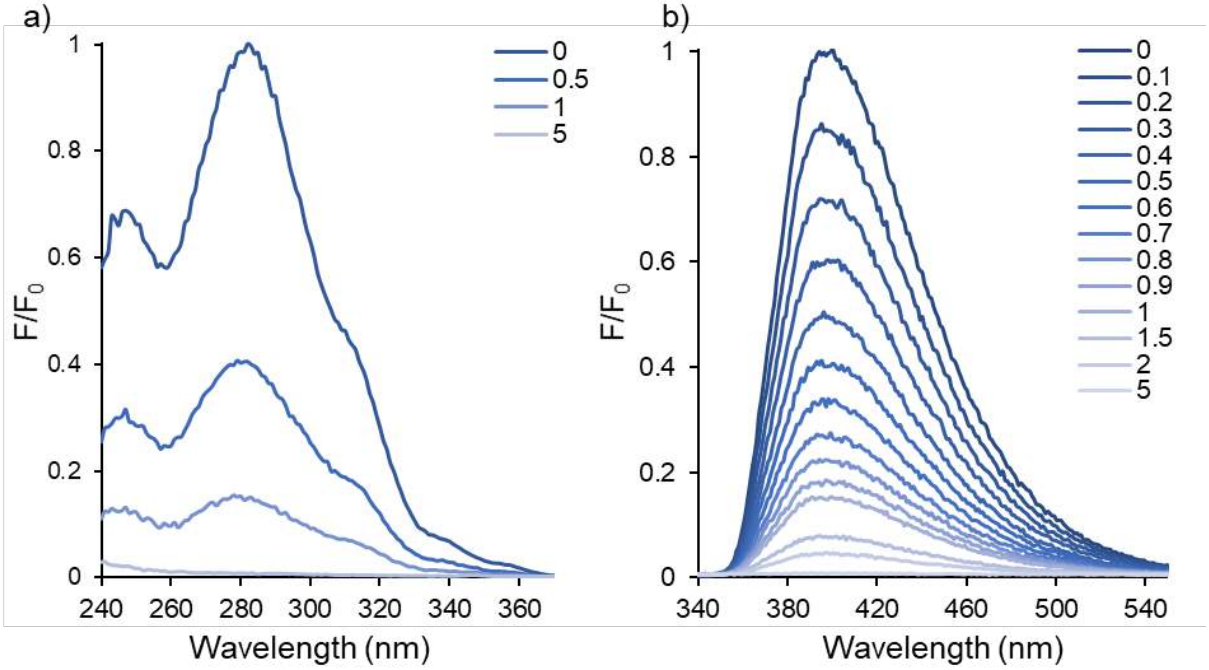

Figure S22. a) Excitation spectra with emission measured at 394 nm and b) Emission spectra with excitation at 282 nm of a 10 µM BCS solution (in a 50 mM sodium phosphate buffer at pH 7) titrated with a solution of 50 µM $CuCl_2$ and 100 µM sodium ascorbate (in a stock solution of BCS). The added amount is expressed in number of equivalents of Cu^+ relative to BCS.

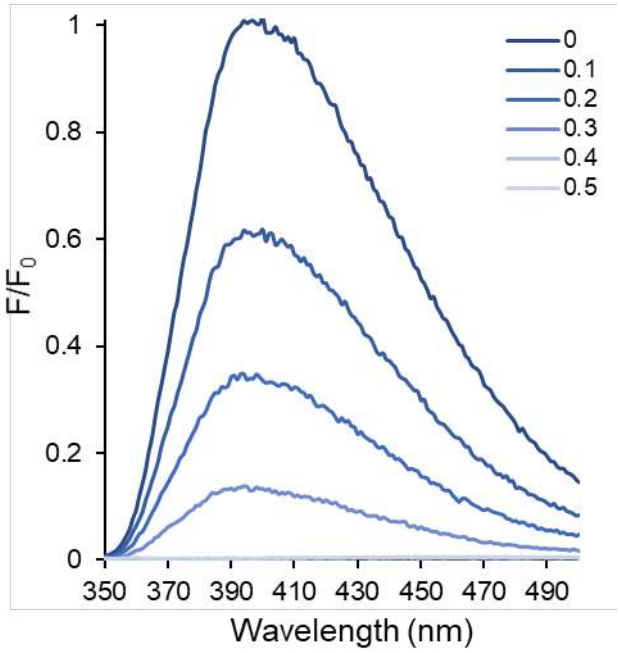

Figure S23. Emission spectra upon excitation at 282 nm of a 0.1 mM BCS solution (in a 50 mM sodium phosphate buffer at pH 7) titrated by a solution of 0.5 mM $CuCl_2$ and 1 mM sodium ascorbate (in a stock solution of BCS). The added amount is expressed in number of equivalents of Cu^+ relative to BCS.

The titrations of BCS with Cu^+ were performed with BCS concentrations either of 10 µM or 100 µM. A faster decrease of the fluorescence intensity was found at higher BCS concentration. With 0.5 equivalent of Cu^+, the fluorescence intensity of 0.1 mM BCS decreased to zero (Figure S23), which is in agreement with the formation of a 2:1 BCS:Cu(I) complex.

4. Transport studies in vesicles by fluorescence assays

4.1. BCS assay - experimental procedure

Stock solution of lipids and calixarene were prepared using deacidified $CHCl_3$ and stored in a freezer. $CHCl_3$ was deacidified by passing through activated basic alumina. The lipids used in order to prepare the liposomes are 2-oleoyl-1-palmitoyl-sn-glycero-3-phosphocholine (POPC), (purity ≥ 99%), dipalmitoylphosphatidylcholine (DPPC), (purity ≥ 99%), and cholesterol (purity of 95%). The aqueous solutions were prepared with milipore water. 50 mM potassium phosphate and 50 mM sodium phosphate buffer were prepared at pH 7 (± 0.1) by mixing the solution of the mono- and the diprotonated phosphate salts. The Cu^+ solutions were obtained by dissolving 0.5 mM $CuCl_2$ (or $CuSO_4$) in a solution of 1 mM sodium ascorbate in phosphate buffer. The copper solutions were freshly prepared for each experiments. The solutions of the dye (BCS) were prepared at 0.5 mM concentration in phosphate buffer.

Fluorescence measurements were performed with a Horiba FluoroMax 4 spectrometer using a 4-faced quartz cuvette (10 mm x 10 mm). For the Cu^+ transport assay monitored with BCS, the excitation was set at 278 nm and emission was recorded at 393 nm, with an opening for both excitation and emission slits of 3 nm and an integration time of 0.2 seconds. These values correspond to the excitation and emission maxima of BCS encapsulated inside LUVs.

The calixarene and lipids solutions were mixed in different ratios in a 5 mL round bottom flask. The POPC/cholesterol molar ratio was 7:3 in all experiments and the ratio of calixarene to lipid was varied from 1/200 to 1/10000. For each set of conditions two batches of liposomes were made: one prepared with the transporter of choice, the other without transporter. The total amount of lipids per batch was varied, depending on the amount of liposome solution required for the experiment. The chloroform was evaporated under a gentle air flow and the resulting lipid film was dried at high vacuum for at least an hour. 500 µL of the dye solution in phosphate buffer and a magnetic stir bar were added to the flask. The flask was then sonicated for 30 seconds and placed under magnetic agitation for at least an hour. The solution was frozen with liquid nitrogen and heated back to room temperature with warm water ten times to form large unilamellar vesicles (LUVs). The solution was then transferred from the flask to the syringe of an extrusion kit, the flask was rinsed with about 0.5 mL phosphate buffer in order to reach a total volume of 1 mL in the syringe. The liposome solution was extruded 29 times, using an extrusion kit equipped with a membrane with 200 nm pores. Subsequently, the solution was eluted with the buffer solution used for the experiment through a size exclusion column (Sephadex G-25) to remove the external BCS and then diluted with phosphate buffer to obtain a concentration of 0.4 mM in lipids. The size exclusion columns were reused for multiple experiments and abundantly rinsed with distilled water until the eluted solutions were not fluorescent anymore and then with the buffer solution used for following the experiment.

Fluorescence measurements were performed on 2.8 mL of final liposome solutions in a quartz cuvette with stir bar. The temperature of the cuvette holder was controlled with a water bath at 25°C for POPC liposomes. 30 seconds after the start of the fluorescence measurement, 200 µL of the Cu^+ solution was added. Each experiment was repeated 3 times and the fluorescence intensity was followed for at least 10 minutes after the addition of the copper solution.

4.2. Quantification of transport rates

The data shown in Figure 4 and S25-S30 were treated as follows: for each run the initial plateau and the initial vertical drop (due to the binding of the exterior dye with Cu^+ and the dilution, 1-4 seconds after the addition) were removed. Then the signal was normalised by dividing the fluorescence values (F) by the value at t = 0 second (F_0). The average of 3 normalised runs (F/F_0) was then calculated and plotted over time.

Normalised and averaged transport curves were fitted to a single and a double exponential decay function in order to obtain half-lives and initial rates.

$F = y + ae^{-bt}$ → Half-life : $ln(2)/b$

$F = y + ae^{-bt} + ce^{-dt}$ → Initial rate : $I_0 = ab + cd$

a)

Trans porter	Ratio T:L	Half-life (s)	I_0 (s^{-1})
2	1:200	40	0.035
2	1:500	70	0.015
2	1:2000	110	0.006
2	1:5000	140	0.004
2	1:10000	230	0.002
1	1:500	120	0.006
3	1:500	75	0.018

b)

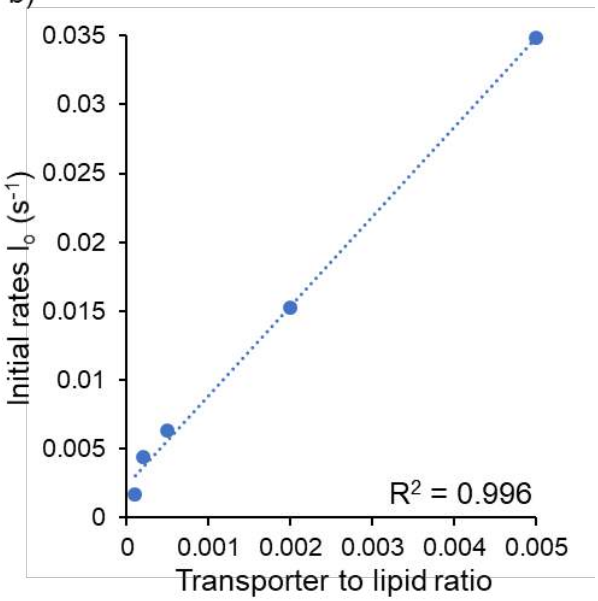

*Figure S24. A) Table of half-lives and initial rates obtained by fitting transport curves of **1**, **2** and **3** at various transporter:lipids (T:L) ratios. b) Linear trend between initial rates of transport by **2** and transporter:lipids ratios.*

4.3. Control experiment: BCS Concentration

A control experiment was conducted to verify that the Cu^+ transport was not impacted by the presence of BCS encapsulated inside the liposomes. As the detection of Cu^+ transport is occurring through a binding process with BCS, transport rates were measured with various concentrations of encapsulated BCS. Initials rates of transport did not show significant change upon increasing the concentrations of BCS, implying that the kinetics of transport of Cu^+ are not significantly influenced by the binding process between Cu^+ and BCS inside the liposomes.

*Table S1. Initial rates obtained by fitting transport curves of **2** (at transporter:lipid ratio 1:500) with different concentrations of BCS encapsulated.*

Transporter	Ratio T:L	BCS concentration (mM)	I_0 (s^{-1})
2	1:500	0.5	0.015
2	1:500	2	0.017
2	1:500	5	0.013

4.4. Control experiment: Copper reducing agent

In situ reduction of Cu^{2+} to Cu^+ was performed by sodium borohydride instead of sodium ascorbate and the results obtained are similar to those with sodium ascorbate.

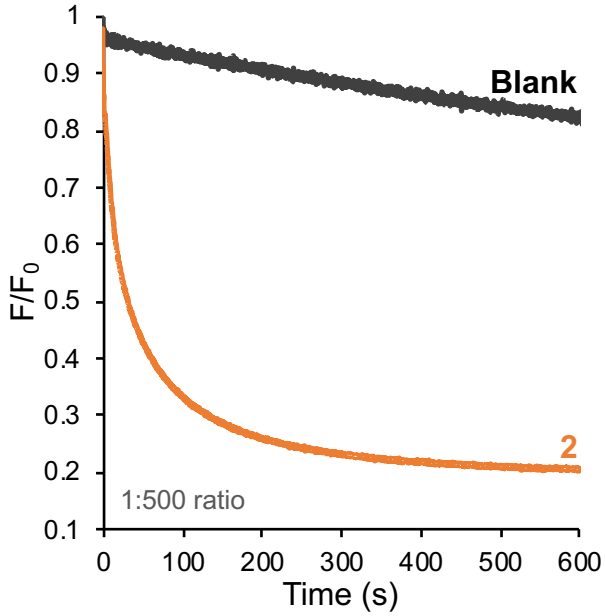

*Figure S25. Comparison between Cu^+ transport curves after addition of $CuCl_2$ mixed with $NaBH_4$ as reducing agent. Transport measurements of Cu(I) by following the decrease of fluorescence of BCS (excitation at 278 nm, emission at 393 nm) encapsulated inside LUVs with **2** (1/500 transporter to lipids ratio) in 50 mM sodium phosphate buffer (pH 7). Addition of 200 µL of a 0.5 mM $CuCl_2$ and 1 mM $NaBH_4$ in 50 mM sodium phosphate buffer (pH 7) to 2.8 mL LUVs (0.4 mM lipids) created a Cu^+ gradient. A blank measurement with $CuCl_2$ an $NaBH_4$ is shown for comparison.*

4.5. Transport of Cu^+ by **2** in DPPC vesicles

The Cu^+ transport ability of **2** was studied with DPPC lipids instead of POPC. The procedure for the preparation of the liposomes was similar to the one described in Section 4.1 with the exception that the hydration and extrusion processes were conducted at temperatures above 45°C, to make sure that the lipids were above the gel transition temperature of DPPC (41°C).

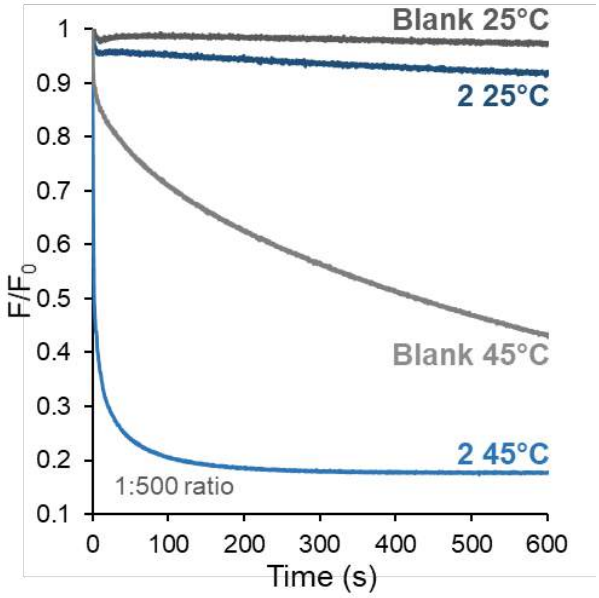

*Figure S26. Comparison between Cu^+ transport curves of **2** above and below the gel transition temperature of DPPC lipids. Transport measurements of Cu(I) by following the decrease of fluorescence of BCS (excitation at 278 nm, emission at 393 nm) encapsulated inside LUVs with **2** (1/500 transporter to lipids ratio) in 50 mM sodium phosphate buffer (pH 7). Addition of 200 μL of a 0.5 mM $CuCl_2$ and 1 mM sodium ascorbate in 50 mM sodium phosphate buffer (pH 7) to 2.8 mL LUVs (0.4 mM lipids) created a Cu^+ gradient. Blank measurements are shown for comparison.*

At 25°C, the membrane is in a gel phase and no transport was observed. However, at 45°C, the lipids are in a fluid phase, allowing molecules inside the membrane to diffuse and transport abilities were retrieved (Figure S26).This indicates that calixarene **2** functions as a mobile carrier, similar to cationophores valinomycin and monensin, and not as a channel.[v] This carrier mechanism is consistent with the fact that calixarene **2** is too small to span the bilayer and there are no reasons for multiple molecules to interact and form a channel, as shown by the concentration dependence experiments (see Section 4.2). It is unlikely that expulsion from the membrane is the cause of the absence of transport activity in DPPC at 25°C,[vi] considering the high lipophilicity of **2** (logP ≈ 17) and the efficient retrieval of transport above the gel phase transition temperature.

4.6. Transport of Cu^+ by **2**: experiments with different salts

To further study the Cu^+ transport mechanism, experiments with slight variations to the protocol described in Section 4.1 were performed. The Cu^+ salts used to trigger the transport were changed from $CuCl_2$ to $CuSO_4$ (and combined with sodium ascorbate, as before) to evaluate potential co-transport of ion pairs. In another experiment, the cation of the phosphate buffer solution was changed from sodium to potassium in order to evaluate potential antiport with Cu^+.

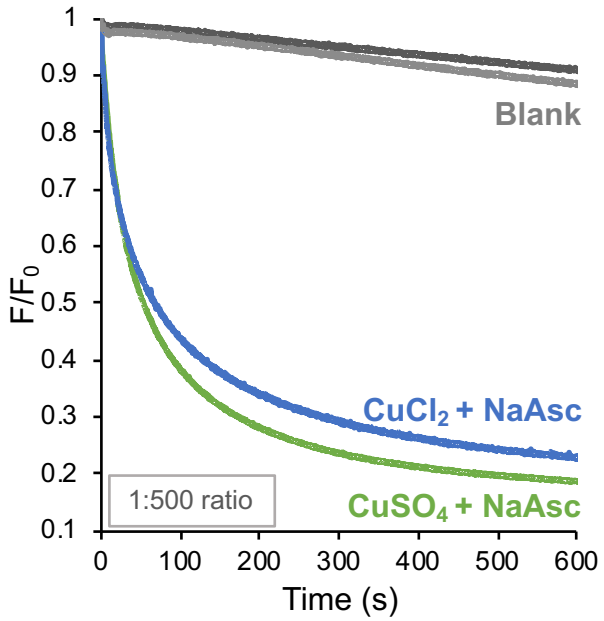

*Figure S27. Comparison between Cu^+ transport curves after addition of $CuCl_2$ or $CuSO_4$ both mixed with sodium ascorbate. Transport measurements of Cu(I) by following the decrease of fluorescence of BCS (excitation at 278 nm, emission at 393 nm) encapsulated inside LUVs with **2** (1/500 transporter to lipids ratio) in 50 mM sodium phosphate buffer (pH 7). Addition of 200 µL of a 0.5 mM $CuCl_2$ or $CuSO_4$ or and 1 mM sodium ascorbate in 50 mM sodium phosphate buffer (pH 7) to 2.8 mL LUVs (0.4 mM lipids) created a Cu^+ gradient. A blank measurement with $CuCl_2$ an sodium ascorbate is shown for comparison.*

The rates of transport with $CuSO_4$ and sodium ascorbate were similar to those with $CuCl_2$ and sodium ascorbate. It is thus unlikely that the counter anion is co-transported with Cu^+, as significantly different rates of transport would be expected due to the high charge and hydration energy of SO_4^{2-} (- 1059 kJ mol^{-1}) compared to Cl^- (- 381 kJ mol^{-1}).[vii]

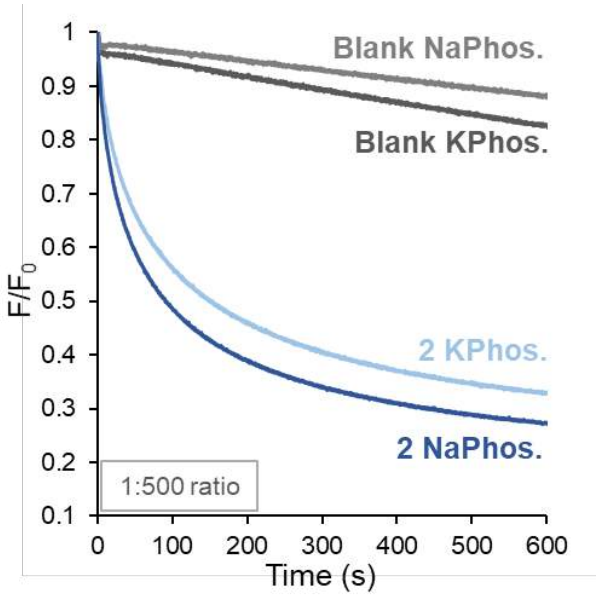

*Figure S28. Comparison between Cu^+ transport curves of **2** in Na and K phosphate buffer. Transport measurements of Cu(I) by following the decrease of fluorescence of BCS (excitation at 278 nm, emission at 393 nm) encapsulated inside LUVs with **2** (1/500 transporter to lipids ratio) in 50 mM phosphate buffer (pH 7). Addition of 200 μL of a 0.5 mM $CuCl_2$ and 1 mM sodium ascorbate in 50 mM phosphate buffer (pH 7) to 2.8 mL LUVs (0.4 mM lipids) created a Cu^+ gradient. Blank measurements are shown for comparison.*

The rates of transport in a sodium phosphate buffer were only slightly faster than in potassium phosphate buffer, and the difference is not significant. Indeed, the half-life of the transport curves was 85 seconds in the potassium phosphate buffer compared to 70 seconds in the sodium one. These results do not hint an anti-transport mechanism with either sodium or potassium.

4.7. Transport H^+, K^+ and Na^+ by **2**: HPTS measurements

As demonstrated in Section 4.6, Cu^+ transport is not occurring through symport with anions. Another hypothesis could be antiport of Cu^+ with another cation. Even though the data in Figure S28 do not indicate such mechanism, the equal rates of transport in sodium and potassium phosphate do no completely rule out the transport of Na^+ and K^+ either. Therefore, the ability of **2** to transport and/or exchange H^+, Na^+ or K^+ was studied using the commonly used dye HPTS.[viii]

The protocol used for the preparation of liposomes with HPTS is similar to the one described in Section 4.1. A solution of the pH sensitive dye 8-Hydroxypyrene-1,3,6-Trisulfonic Acid (HPTS, 1 mM), was added to hydrate the lipid films instead of a solution of BCS. All solutions were prepared in a 10 mM Na^+ or K^+ phosphate buffer at pH 7 (± 0.1). The proton gradient was induced by addition of 30 µL NaOH or KOH (0.5 M) to 3 mL liposomes. After ~ 12 minutes, the liposomes were lysed by adding 50 µL of Triton X-100 (5% m/m in water).
In some measurements valinomycin and/or carbonylcyanide *m*-chlorophenylhydrazone (CCCP) were used as ways to provide pathways for respectively K^+ or H^+ transport. Stock solutions of both transporters were prepared in MeOH at a 0.24 mM concentration, 5 µL of which was added to 3 mL of liposome solutions (1:1000 transporter to lipid ratio) and left to stir for 5 minutes before starting the transport experiments.
The pH was followed by measuring the emission of the liposome solution at 510 nm when alternatively exciting at 403 nm and at 454 nm, with all slits openings set at 1 nm. The fluorescence intensity obtained when exciting at 454 nm is divided by the one obtained when exciting at 403 nm, and the ratio is then plotted over time. For each experiments, three transport curves were recorded and normalized from 0 to 1, with the starting level set at zero and the lysing level set at 1. The data shown in figure S29-S30 are the average of the three normalized transport curves.

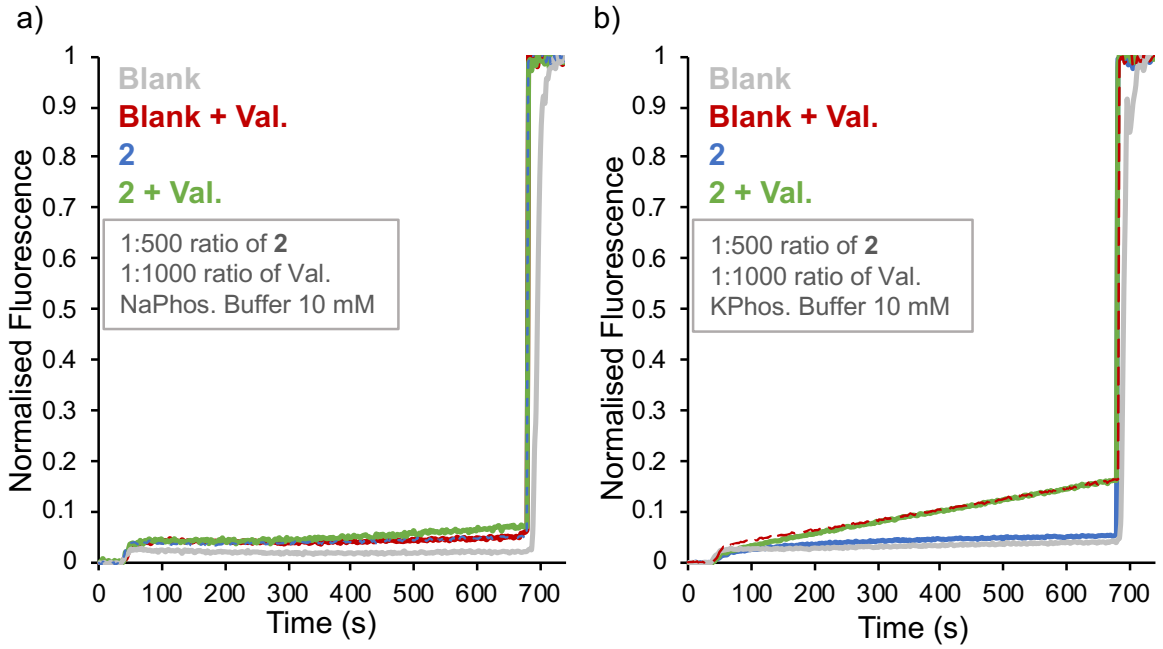

*Figure S29 Transport measurement of H^+ by following the increase of fluorescence ratio of HPTS (alternative excitation at 503 and 545 nm, emission at 510 nm) encapsulated inside LUVs with **2** (1/500 transporter to lipids ratio) in 10 mM sodium (a) potassium (b) phosphate buffer (pH 7). Addition of 30 µL of a 0.5 M NaOH (a) KOH (b) after 30 seconds to 3 mL LUVs (0.4 mM lipids) created a pH gradient. Addition of 50 µL of Triton x-100 (5%) 30 seconds before the end of the experiment. Blank (no transporters) and valinomycin only (5 µL at a 0.24 mM concentration in MeOH) measurements are shown for comparison.*

The results in Figures S29 (blue curves) show that **2** was unable to transport H^+ by exchange with either Na^+ or K^+ (antiport mechanism), when a pH gradient was applied.
Upon addition of cationophore valinomycin in K^+ phosphate, slow transport of H^+ was observed. This was attributed to the activity of valinomycin, as transport curves with and without **2** are similar (green and red). Because the combination of valinomycin and **2** did not give any significant H^+ transport, we can conclude that **2** is also not able to transport H^+ by a uniport mechanism.

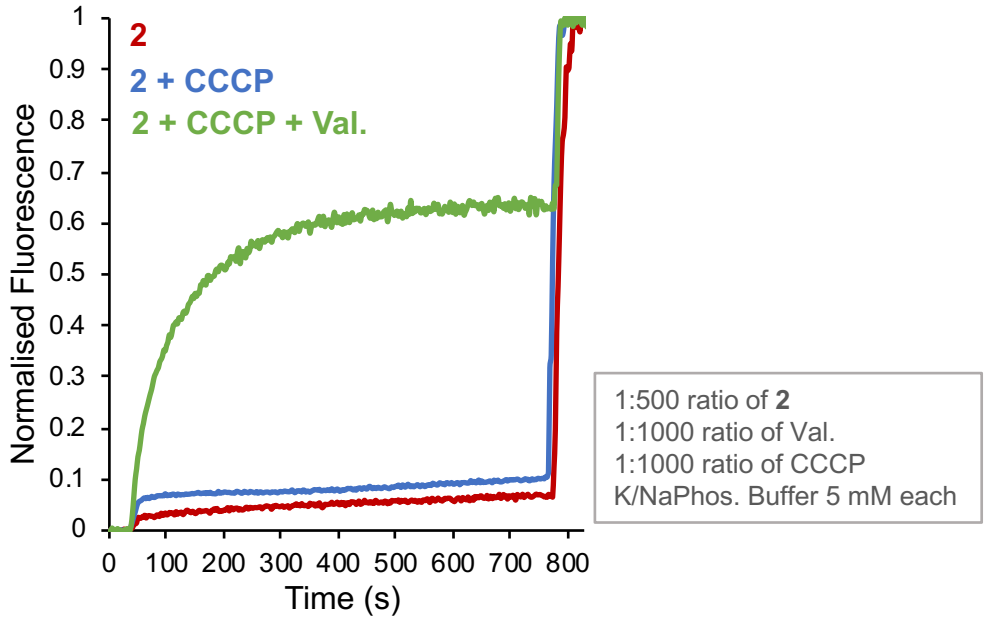

*Figure S 30 Transport measurements of H^+ by following the increase of fluorescence ratio of HPTS (alternative excitation at 503 and 545 nm, emission at 510 nm) encapsulated inside LUVs with **2** (1/500 transporter to lipids ratio) in 10 mM phosphate buffer (pH 7). Addition of 30 µL of a mixture of 0.25 M NaOH and 0.25 M KOH (50/50) after 30 seconds to 3 mL LUVs (0.4 mM lipids) created a pH gradient. Addition of 50 µL of Triton x-100 (5%) 30 seconds before the end of the experiments. Blank, CCCP and valinomycin (5 µL at a 0.24 mM concentration in MeOH) measurements are shown for comparison.*

Having found that **2** is incapable of transporting H^+ by either uniport or symport mechanisms, further experiments were performed to study the ability of **2** to transport Na^+ or K^+ by a uniport mechanism. This was tested by addition of protonophore CCCP, which would allow the transport of H^+ in the HPTS assay.
However, addition of CCCP did not improve the transport by **2** in the HPTS assay (Figure S30, blue curve). The H^+ transport activity of CCCP was limited by the accumulation of membrane potentials between the interior and exterior of the membrane due the inability of **2** to transport either Na^+ or K^+ by uniport. In presence of valinomycin the H^+ transport ability of CCCP was clearly observed (Figure S30, green curve), highlighting that the membrane potential gradient build up was indeed limiting the protonophoric activity of CCCP.

Considering that **2** is unable to transport Na^+ or K^+, either by uniport or by exchange it with H^+ (symport), we conclude that Cu^+ transport by an antiport mechanism with Na^+ or K^+ is highly unlikely.
This means that the Cu^+ transport appears to happen without compensation of charge. The relatively small Cu^+ concentration gradient results thus in the gradual building-up of a potential gradient across the membrane of the liposomes upon Cu^+ transport. Attempts to monitor this potential gradient with the dye Safranin O were not successful, due to the small concentration of Cu^+ involved.

5. U-tube experiment

5.1. Experimental procedure

4 mL of $CHCl_3$ was introduced into a U shaped glassware. On each side of the $CHCl_3$ phase, an aqueous solution was added, one with Cu^+ and the other one without Cu^+. For the donor phase (D) 5 mL of a suspension of 0.5 mM of $CuCl_2$ and 1.0 mM sodium ascorbate was added whereas for the receiving phase (R) only water was added. Two experiments were performed, one in which the $CHCl_3$ contains 1 mM of **2**, the other one in absence of a transporter (blank). The $CHCl_3$ phase was magnetically stirred.

0.5 mL of both aqueous solutions (R and D) were removed at the beginning of the experiment and after 3, 5, and 7 days of stirring. 1 mL of a 5 μM BCS solution was added to each of the 0.5 mL samples. The fluorescence intensity of the mixture was measured at 394 nm when exciting at 278 nm. In order to evaluate the amount of Cu^+ transported, a titration of BCS (3.33 μM in H_2O) was conducted with identical settings of the fluorescence spectrometer.

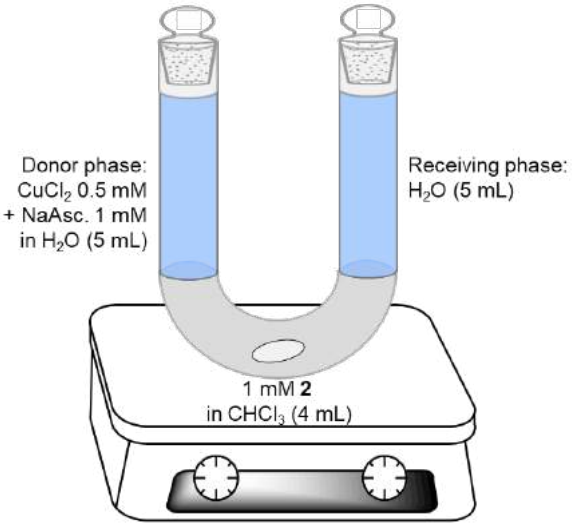

Figure S31. Experimental setup of U-tube experiments

5.2. Results

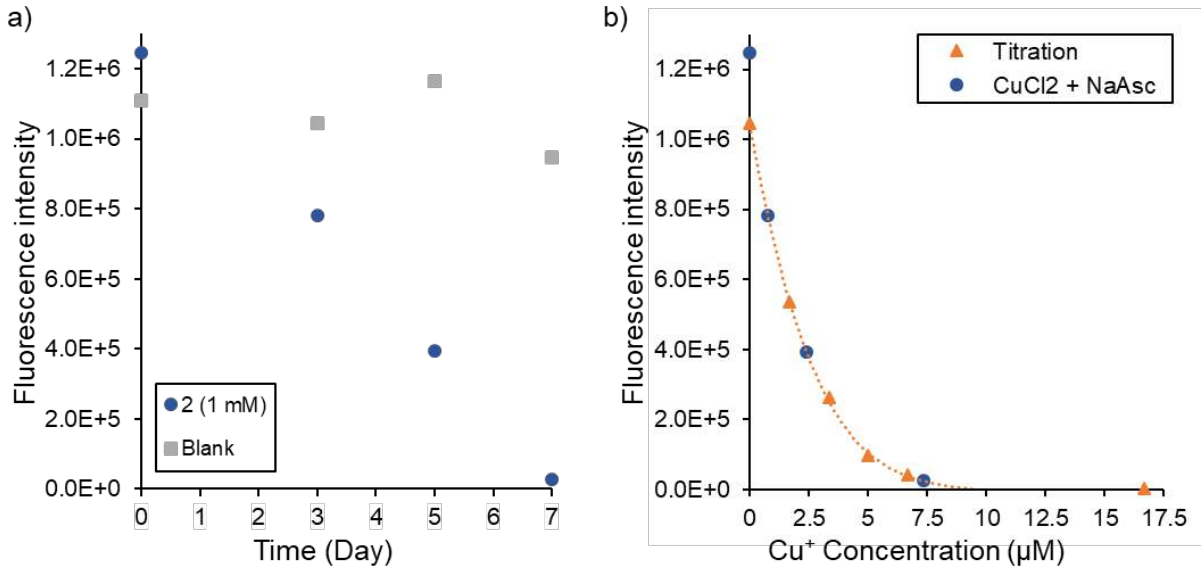

Figure S32. a) Fluorescence of 1 mL of BCS (5 µM) mixed with 500 µL of the receiving phase of the U-tube experiments with excitation at 278 nm, emission at 394 nm. The U-tube were set up with ***2*** *(1 mM) and without transporter (blank) in $CHCl_3$ with an aqueous phase on either side. The measurements were followed during 7 days of continuous stirring; b) Emission intensity at 394 nm of a 3.33 µM BCS solution titrated by a solution of 0.5 mM $CuCl_2$ and 1 mM sodium ascorbate (in a stock solution of BCS). The results from the U-tube experiments are plotted on the titration curve and correspond to a third of the Cu^+ concentration in the receiving phase of the U-tubes.*

The concentration of Cu^+ in the receiving phase of the U-tube containing **2** increased over time to reach ~22 µM after 7 days, which is about 4% of the initial Cu^+ concentration in the donor phase, whereas the concentration of Cu^+ in the receiving phase of the blank experiment did not increase significantly.

6. References

[i] L. L. Clainche, M. Giorgi, O. Reinaud, *Eur. J. Inorg. Chem.* **2000**, *2000*, 1931–1933.
[ii] K. Iwamoto, K. Araki, S. Shinkai, *J. Org. Chem.* **1991**, 56 (16), 4955–4962
[iii] S. G. Bott, A. W. Coleman, J. L. Atwood, *J. Am. Chem. Soc.* **1986**, *108* (7), 1709–1710.
[iv] Bindfit 1:1 binding model on http://supramolecular.org/
[v] J. L. Seganish, J. T. Davis, *Chem. Commun.* **2005**, 5781.
[vi] S. Otto, M. Osifchin, S. L. Regen, *J. Am. Chem. Soc.* **1999**, *121*, 10440–10441.
[vii] D. W. Smith, *J. Chem. Educ.* **1977**, *54* (9), 540.
[viii] N. Sakai, S. Matile, *J. Phys. Org. Chem.* **2006**, *19* (8–9), 452–460.